A Combined Hydrologic/Geochemical Investigation of Groundwater Conditions in the Waukesha County Area, WI

Tim Grundl[1], Ken Bradbury[2], Daniel Feinstein[3], Sue Friers[1], Dave Hart[2]

[1] Geosciences Department, University of Wisconsin-Milwaukee
[2] Wisconsin Geological and Natural History Survey and University of Wisconsin-Extension
[3] United States Geological Survey

Final Report submitted to Wisconsin Groundwater Research Program at completion of grant number WR03R002

Table of Contents

Introduction

This report describes work done to ascertain the overall flow and geochemical conditions within the deep sandstone aquifer of southeast Wisconsin. The study focused particularly on Waukesha county, an area that is experiencing severe overpumping of the aquifer and contains several wells that produce water with radium activities in excess of the USEPA mandated limit of 5 pCi/L total radium. The affected municipalities are facing the possibility of EPA imposed fines, of installing expensive water treatment procedures or developing an alternate source of radium-free water. An understanding of radium behavior in this aquifer is very important to the affected communities.

High radium activities in Waukesha county occur along a band roughly parallel to and east of the Maquoketa subcrop. Previous workers were able to show that the generally low radium activities found in the aquifer to the west of the Maquoketa subcrop are controlled by co-precipitation into barite, but could not identify the cause of high activities found east of the subcrop (Grundl and Cape, 2006). This report is an extension and refinement of several earlier studies completed in southeastern Wisconsin (Clayton, 1999; Schmidt, 2002; Feinstein, et al., 2005; Grundl and Cape, 2006;). The overall hydrologic/geochemical conditions established in these earlier studies are used as a backdrop for a detailed investigation into the causes behind the high radium activities (in excess of 5 pCi/L) found east of the Maquoketa subcrop in Waukesha county. A final outcome of this work is the delineation of an isotopic and noble gas signature of these waters that is indicative of Pleistocene recharge. Implications as to the age and recharge dynamics beneath glaciated sediments are discussed.

Project Approach

The federally-mandated limit of 5 pCi/L of radium in drinking water represents a vanishingly small concentration of radium ions in the water. Five pCi/L is equivalent to $5x10^{-9}$ ppm (^{226}Ra) or $2x10^{-11}$ ppm (^{228}Ra). Unraveling the behavior of these ultra-trace ions in the context of a regional aquifer system is a daunting task that depends upon a

clear understanding of both the physical and chemical dynamics of the aquifer itself. In pursuit of this goal, this project took advantage of the fact that a large amount of information was already available including previous regional geochemical studies, an extensive groundwater flow model of the entire region, and chemical data from over 50 wells in Waukesha county alone. The intellectual approach taken was to first assemble the previously available regionalized data and apply it to the Waukesha county area specifically. This effort was undertaken to understand the generic flow and chemical conditions currently in existence in the aquifer. It focused on using the regional ground water flow model to assess details of the flow regime within Waukesha county as well as collecting and modeling the major ion data that resides in the Wisconsin Department of Natural Resources (WDNR) drinking water data base. Secondly, a series of individual investigations was undertaken to assess the efficacy of specific processes that could supply radium to aquifer water. This included investigations into the mineralogy of aquifer solids, colloidal material, radium versus depth relations and radium versus vertical head relations. Thirdly, isotope and noble gas techniques were employed to refine the understanding of aquifer dynamics over long periods of time (thousands of years). This was needed in order to be confident extrapolating currently active processes into the past. The result is a cohesive picture of the aquifer dynamics obtained by applying a wide variety of tools, including numerical flow modeling, geochemical modeling (based on both major ion chemistry and solids information), isotope and noble gas data.

Hydrogeologic conditions

The physiographic setting of southeastern Wisconsin is typical of glaciated landscapes in the northern Midwest. An unconsolidated surficial veneer of Quaternary deposits overlies the eroded bedrock (Mickelson et. al., 1984; Young, 1992). Regional bedrock consists of a cyclic, transgression-regression sequence of marine sedimentary rocks deposited by the epeiric seas of the Lower Paleozoic era. These sedimentary units overlie a Pre-Cambrian basement composed of granites, quartzites, and slates. The bedrock units dip radially from the Wisconsin Arch, a structural high of the Pre-Cambrian basement centered in Wisconsin, eastward towards the Michigan Basin and

southward towards the Illinois Basin. The bedrock geology of southeastern Wisconsin is shown in Figure 1 (modified from WGNHS, 1995)

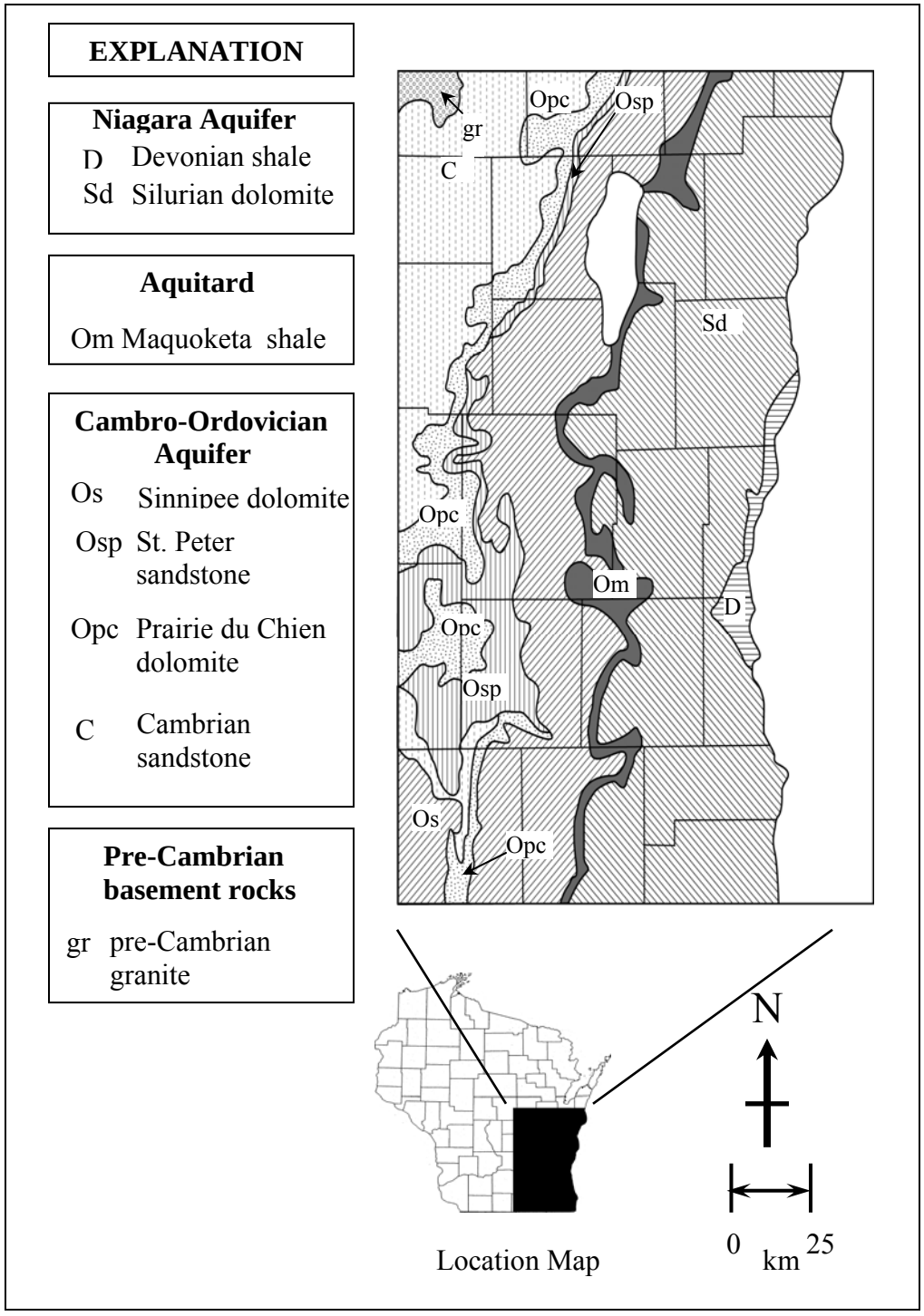

Figure 1: Bedrock geology of southeastern Wisconsin.

The hydrogeologic system of southeastern Wisconsin is comprised of both unconsolidated Quaternary deposits and Paleozoic bedrock strata. The system is categorized into three major hydraulic units, in descending order: 1) the shallow aquifer; 2) the Maquoketa and Sinnippee Formation aquitard; and 3) the deep, Cambrian-Ordovician aquifer (Feinstein, et al., 2005). The contact with essentially impermeable Pre-Cambrian basement rock acts as the basal boundary of the system. The shallow aquifer is unconfined, consisting of unconsolidated Quaternary deposits and the uppermost bedrock units (Silurian and Devonian dolomites). Where the Maquoketa aquitard exists, it confines the underlying Cambrian-Ordovician aquifer and separates it from the shallow aquifer. Regionally, the unit acts as a major hydraulic barrier, limiting the transfer of water between the shallow and Cambrian-Ordovician aquifers. The Maquoketa thins as the western edge is approached and its confining capability diminishes. Near the Maquoketa boundary the aquifer transitions from fully confined to semi-confined conditions (Feinstein, et al., 2004). West of the Maquoketa boundary the shallow and the Cambro-Ordovician aquifers are hydraulically connected.

It has long been known that the Cambrian-Ordovician aquifer is unconfined to the west of the Maquoketa boundary along the entire Lake Michigan coastline throughout Wisconsin and Illinois and that the primary recharge area lies to the west of the boundary (Gilkeson et al., 1984; Siegel, 1990; Weaver and Bahr, 1991b). Recent modeling work by Feinstein, et al. (2005) in southeastern Wisconsin has further defined the flow regime of this aquifer. Small, local flow cells dominate the flow regime to the west of the Maquoketa subcrop boundary and water is freely exchanged between the Cambro-Ordovician aquifer and the overlying aquifer and surface water. The aquifer transitions to confined conditions east of the Maquoketa subcrop and the flow regime changes markedly to a system of uniform, lateral flow toward and eventually into Lake Michigan which serves as the regional sink for ground water flow. Exchange with overlying aquifers and surface water bodies is very limited east of the Maquoketa subcrop. Prior to large scale pumping, the ground water divide generally coincided with the Maquoketa subcrop. Under current conditions, large municipal pumping centers have caused regional cones of depression to develop. The largest pumping center and the deepest cone of

depression is centered east of the Maquoketa subcrop in east-central Waukesha county. The current cone of depression is about150 meters deep.

Large scale pumping has shifted the deep ground water divide to the west by approximately 17 km. Even in the vicinity of large pumping centers, local flow cells dominate west of the ground water divide and lateral flow still dominates to the east. However ground water no longer flows uniformly to Lake Michigan but rather towards the center of pumpage. In areas that lie between the cone of depression and Lake Michigan this has reversed the direction of ground water movement (Feinstein, et al., 2005). Kenosha county and portions of Walworth county are currently under the influence of Chicago's cone of depression and a separate groundwater divide occurs between the two cones. Figure 2 shows the flow regime before and after large scale pumping was impressed upon the aquifer (modified from Feinstein, et al., 2005).

Because of the presence of the Maquoketa shale, downward leakage to the confined portion of the aquifer is mostly from the unconfined portion immediately west of the Maquoketa subcrop boundary. Figure 3 is a modeled cross sectional view of the aquifer along an east-west transect (denoted in Figure 2) showing preferential downward leakage near the westernmost extent of the Maquoketa shale (modified from USGS 2006).

West of the Maquoketa subcrop the aquifer is in hydraulic contact with surface water and the flow is dominated by local flow cells, one of which is visible in Figure 3. The unconfined portion of the aquifer is also more rapidly flushed than the confined portion and this causes significant differences in the groundwater chemistry in both places. Although the aquifer is stratigraphically continuous, it is hydraulically distinct east and west of the Maquoketa subcrop. This hydraulic distinction was in place before large scale pumping began.

pre-pumpage flow pattern ***present day flow pattern***

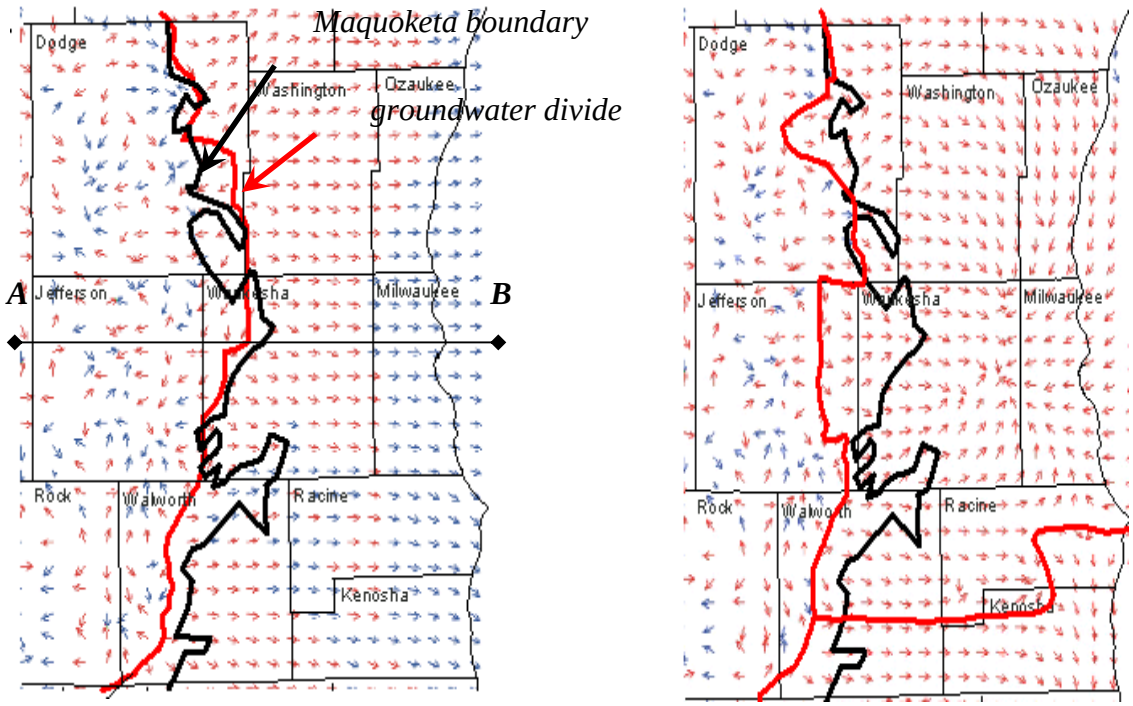

Figure 2: Modeled groundwater flow lines before and after large scale pumping was impressed upon the aquifer. Modeled horizon is in the St. Peter sandstone toward the top of the deep Cambro-Ordovician aquifer. Blue arrows indicate upward flow. Red arrows indicate downward flow.

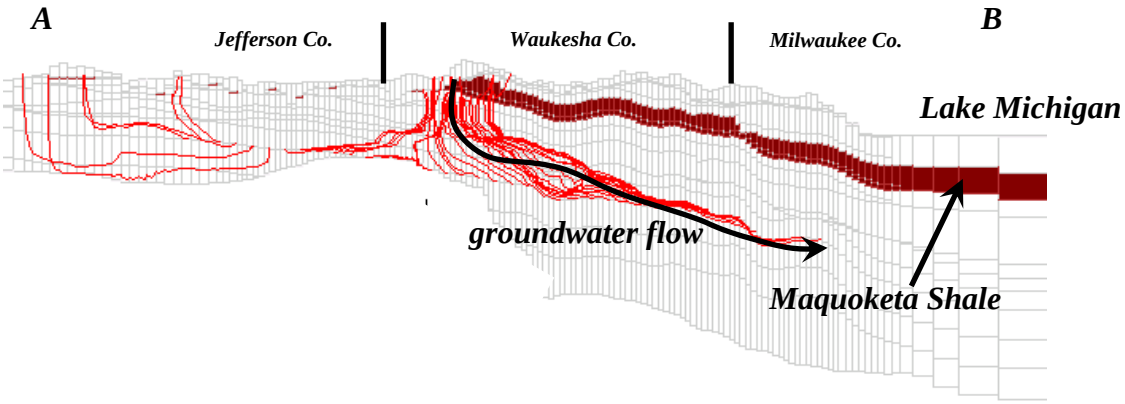

Figure 3: East-west transect across Jefferson, Waukesha and Milwaukee counties. Modeled flow lines that extend from entry to the water table as recharge to selected cells within the St. Peter sandstone are shown with thin (red) lines. Thick (black) arrow shows the general flow direction in the confined portion of the aquifer. Transect location is shown in Figure 2.

Recent large scale pumping has not only caused a large and ever deepening cone of depression, but has also altered the rate of groundwater flow through the aquifer. Figure 4 depicts the modeled specific flux for both pre-pumping and current conditions. Specific flux is given in terms of volume water moved /volume aquifer/1000 years. Under pre-pumpage conditions the steady eastward flow of confined water under the Maquoketa shale is quite slow (specific flux between 0.04 and 0.54). Assuming an effective porosity of 10%, this represents only 0.4 to 5.4 pore volumes moved/1000 years. This contrasts sharply with current conditions in which portions of the confined aquifer are experiencing specific fluxes as great as 1.94 (19.4 pore volumes/1000 years). This is particularly evident in those portions of the aquifer that lie between the recharge area at the Maquoketa subcrop and the cone of depression centered in eastern Waukesha county. The more rapidly flushed, unconfined portion of the aquifer is evident west of the Maquoketa boundary, especially under pre-pumping conditions.

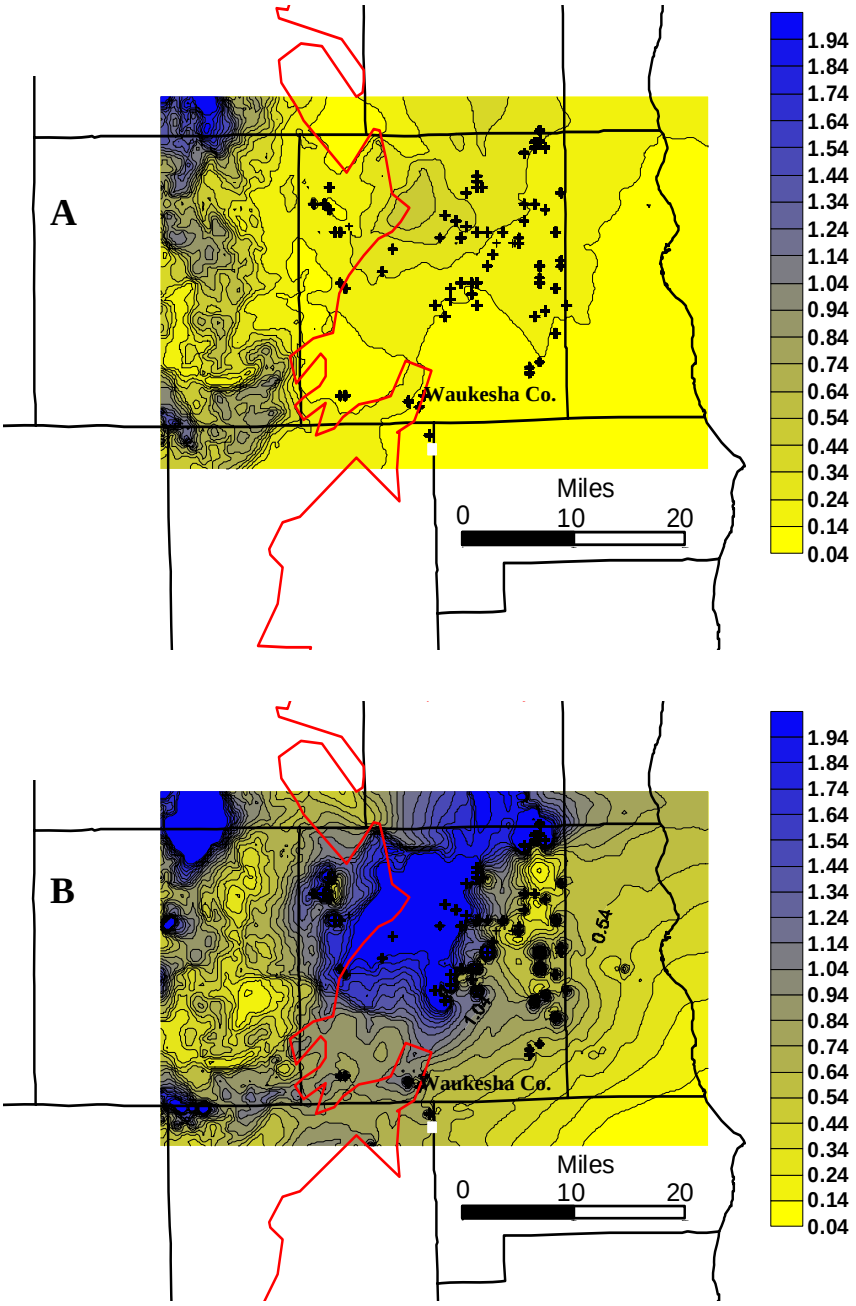

Figure 4: Modeled specific flux values for the deep sandstone aquifer under pre-pumping (A) and current conditions (B). The irregular (red) line through center of figure (red) is the western boundary of the Maquoketa Shale. County boundaries are delineated with straight (black) lines. Specific flux values are given in units of volume water/volume aquifer /1000 years.

Modeled flow rates can be used to estimate the probable age of groundwater reaching wells within the study area. Flow rate estimates depend strongly on the assumed effective porosity. Three sets of assumed effective porosities were used in the development of the regional model as shown in Table 1.

	Assumed effective porosities		
Stratigraphic unit	High	Middle	Low
Unlithified sediments	0.20	0.15	0.05
Silurian dolomite, Maquoketa Shale, Sinnippee dolomite	0.01	0.005	0.005
St. Peter sandstone, Prarie du Chien dolomite and Cambrian Sandstones	0.10	0.02	0.005

Table 1: Three sets of assumed effective porosities used in the regional model.

The travel time to a given well was calculated by placing particles in every model layer penetrated by the well. The particles were tracked backwards to the water table and a travel time assigned to each particle. An average travel time of all the units in the vicinity of each well was then calculated. The simulated flow paths respond to the backward sequence of transient conditions. Maximum pumping corresponds to year 2000, pumping began in 1864, and for up to 10,000 years before 1864 the particle tracking responds to steady-state, pre-pumping conditions. In all cases, modeled travel times are small in the unconfined portion of the aquifer and get increasingly long to the east as flow becomes confined by the Maquoketa shale. High assumed effective porosities (Table 1) yield average groundwater ages greater than 20,000 years in parts of eastern Waukesha and Milwaukee counties. Low assumed effective porosities yield ages that are typically less than 5000 years throughout the study area. Figure 5 shows average travel time to wells as calculated for the middle range effective porosity case.

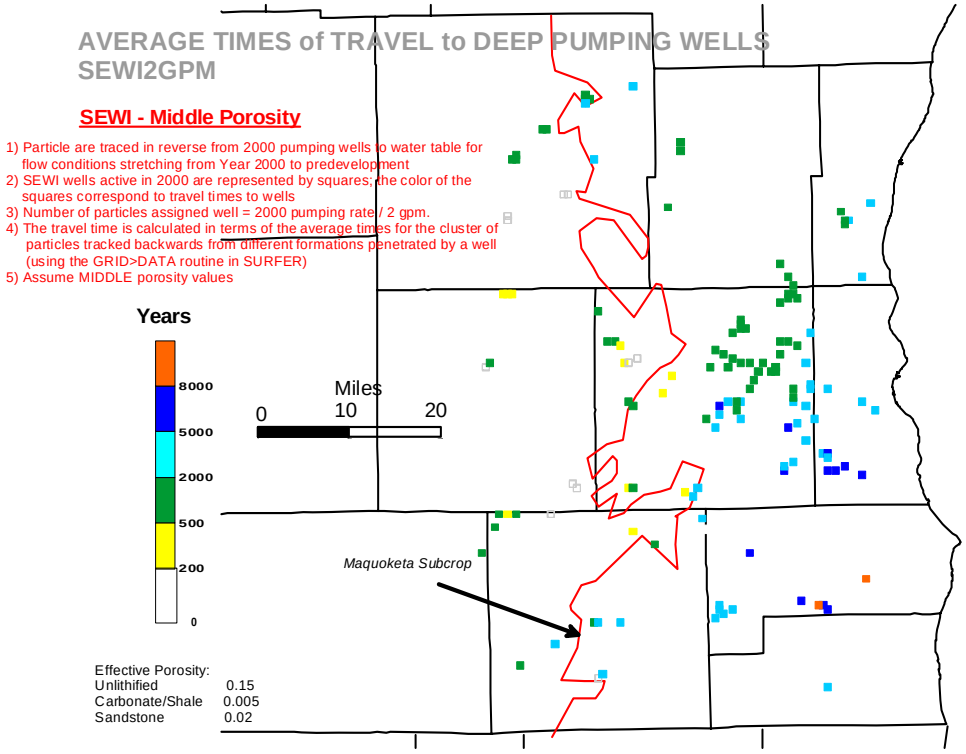

Figure 5: Average travel time to deep sandstone aquifer wells as calculated for the high effective porosity case. Irregular (red) line through center of figure delineates the Maquoketa subcrop. County boundaries are delineated with straight (black) lines.

Geochemical Conditions

The WDNR drinking water database (WDNR, 2005) was used to ascertain the major ion chemistry of the deep sandstone aquifer throughout the whole of eastern Wisconsin. This represents a slight modification of previous work using the WDNR database (Schmidt, 2002). Major ion data was collected from 186 wells that are open solely to the deep sandstone aquifer, charge balance to within 15% and mass balance to within 10%. Previous workers established that major ion chemistry is not changing over period of time for which the WDNR has data (from the mid 1970's to present) (Schmidt, 2002). Therefore multiple analyses from a single well were averaged and treated as a single value. In the vicinity of Waukesha county, unconfined groundwater is strongly Ca-

HCO_3 in nature and becomes more saline as it moves downgradient from the recharge area under the Maquoketa shale largely due to an increase in Ca^{2+} and SO_4^{2-} (Schmidt, 2002). The salinity increases from an average of 425 ppm to 794 ppm as this boundary is crossed. The increase in SO_4^{2-} at the Makoqueta subcrop is evident in Figure 6B. Increasing sulfate causes a shift in the ionic signature from strongly Ca-HCO_3 (>90% HCO_3) chemical character to a more sulfate rich character ($\leq$ 40% HCO_3) (Figure 6A). The change in chemical character coincides with the Maquoketa subcrop as far north as Fond du Lac county where it diverges to the west. This is likely due to the fact that thick Glacial Lake Oshkosh clays form the effective confining layer in this part of the State.

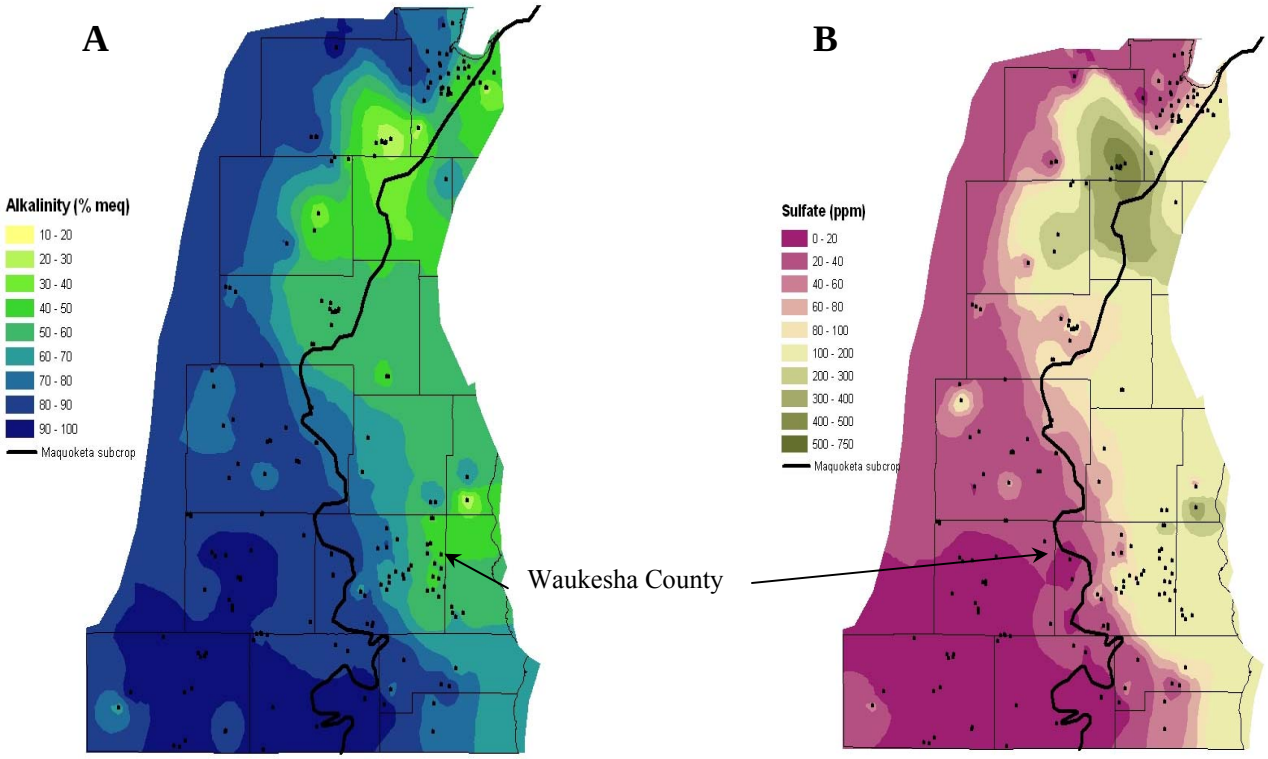

Figure 6: Map of the relative percent alkalinity (A) and sulfate concentrations (B) in the deep sandstone aquifer of eastern Wisconsin. Thick black line is the Maquoketa subcrop. Black spots are the wells from which the map was contoured. County boundaries are delineated with thin black lines. Neither map extends everywhere to the Lake Michigan shoreline because of a lack of data in the northeastern counties.

A Piper diagram of wells in Waukesha county itself show the same trend in detail (Figure 7). Wells in the unconfined portion of the aquifer (red triangles) all produce very similar water with the strong bicarbonate anionic signature and the 50:50 Ca:Mg cationic signature that is expected in a dolomite containing aquifer. The stoichiometric increase in calcium and sulfate in downgradient wells (blue circles and green squares) is most likely from the dissolution of secondary gypsum/anhydrite grains that are distributed throughout the aquifer. Secondary gypsum and anhydrite were emplaced in the aquifer by the dissolution and re-precipitation of Silurian marine evaporite deposits located deep within the Michigan Basin to the east of the study area (Winter et al., 1995). Stable isotope studies of sulfate within the confined portion of this aquifer are consistent with sulfate that originated from seawater-derived evaporites (Siegel, 1990). Earlier studies of the deep sandstone aquifer in northern Illinois and in all of eastern Wisconsin (Perry, et al., 1982) report similar findings. In contrast to conditions seen in northern Illinois, no evidence was found for a low redox zone immediately downgradient of the Makoqueta boundary (Grundl and Cape, 2006). Strontium levels in the confined portion of this aquifer are quite high (averaging 26 ppm) and the importance of strontium is an interesting aspect of the geochemistry of this aquifer. Ionic and radium data for all wells in Waukesha county are given in Appendix C.

In aquifers that are at saturation with respect to calcite, the continuing dissolution of gypsum along the flow path drives a series of sequential reactions (dedolomitization) that lead to the net dissolution of dolomite and net precipitation of calcite. These reactions are:

1) Gypsum dissolution adds Ca^{2+} to the water

2) Additional Ca^{2+} causes calcite oversaturation and the resultant precipitation

3) Calcite precipitation removes CO_3^{2-} from the water causing dolomite undersaturation and the resultant dolomite dissolution.

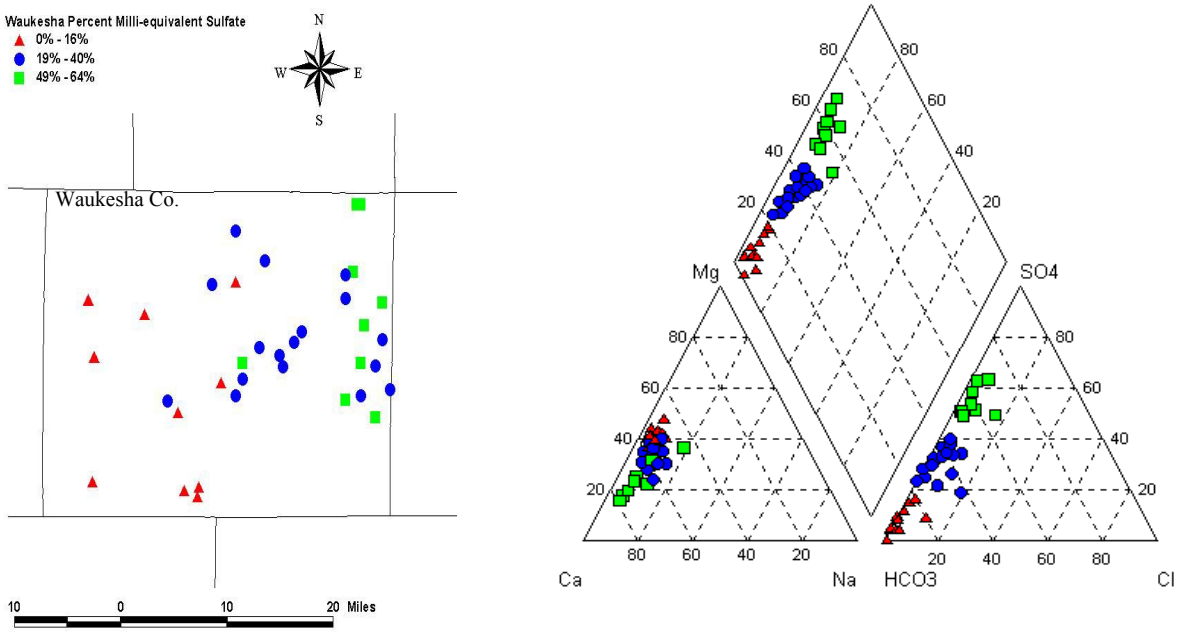

Figure 7: Piper diagram and corresponding location map of deep sandstone wells within Waukesha County. Geochemical evolution towards an increasing calcium and sulfate character (from red triangular through blue circular to green square symbols) follows the general eastward pattern of groundwater flow.

Saturation indices (SI = log [Ksp/IAP] where Ksp is the solubility product and IAP is the ion activity product) derived from PHREEQC modeling provide evidence that dedolomitization is occurring in this aquifer. Saturation indices in Waukesha and Jefferson county wells are plotted versus sulfate concentration in Figure 8. Gypsum is undersaturated by as much as three orders of magnitude in the unconfined, well-flushed portion of the aquifer (all unconfined wells plot to the left of the Makoqueta Shale limit in Figure 8). Gypsum approaches, but never reaches saturation as the Maquoketa boundary is crossed and continuing dissolution of gypsum adds sulfate (to the right of the Maquoketa Shale limit in Figure 8).

Calcite is at saturation in all wells, both confined and unconfined (SI = 0.04 ± 0.25) (± 1 standard deviation) (Figure 8). Dolomite (Figure 8), although more variable, is slightly undersaturated in most wells (SI = -0.22 ± 0.49). Undersaturation with respect to

dolomite is seen in most of the individual samples analyzed by Grundl and Cape (2006). All three SI trends are necessary for dedolomitization to occur.

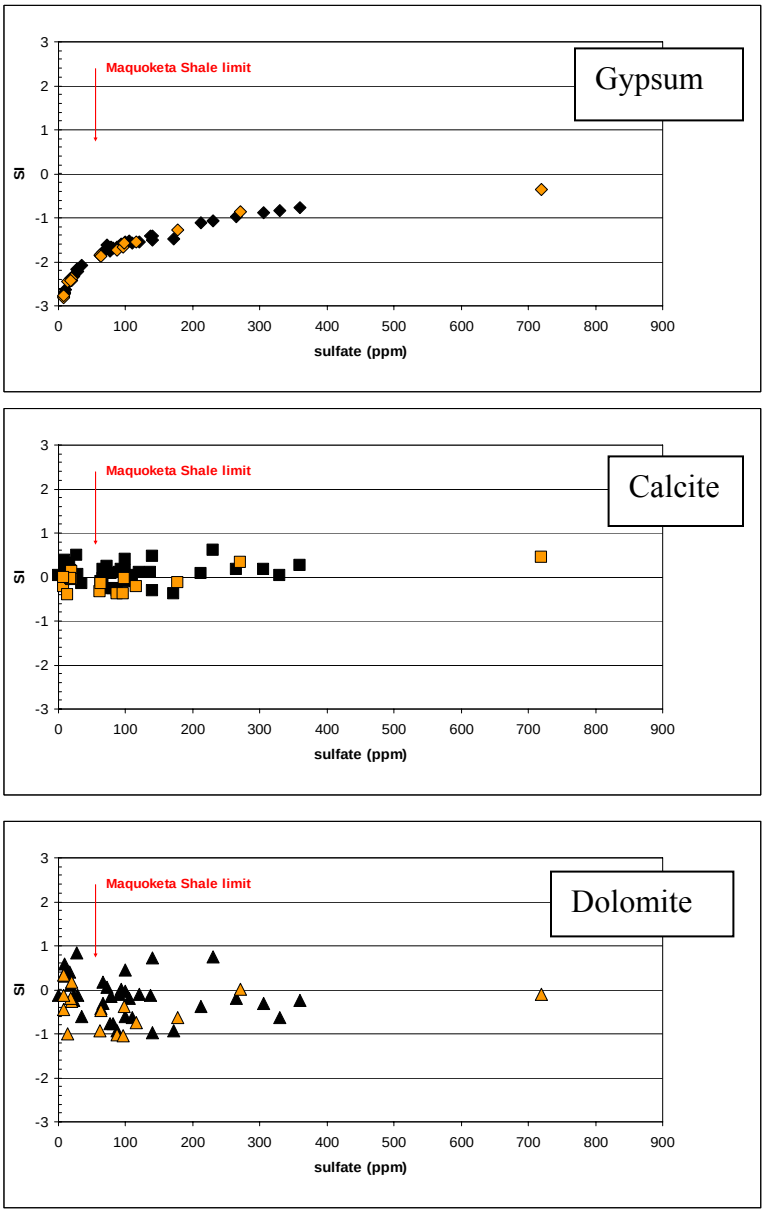

Figure 8: Plot of the PHREEQC calculated saturation indices (SI) for gypsum, calcite and dolomite in Waukesha and Jefferson County wells versus sulfate concentration. Black symbols are calculated from average of multiple samples for a given well as taken from the WDNR database. The lighter (orange) symbols are calculated from individual analyses reported by Grundl and Cape (2006).

The chemical data from which the SI values in Figure 8 are plotted come from two sources; average values of multiple samples for a given well as taken from the WDNR database (black symbols) and values taken from Grundl and Cape (2006) (lighter orange symbols). Grundl and Cape (2006) analyses were taken from single samples taken on the same day and as such are more precise than average WDNR analyses. Much of the imprecision seen in the calcite and dolomite trends is due to the use of averaged WDNR data.

An estimate of the actual mole transfer of mineral phases needed to account for the observed changes in water chemistry along the flow path can be made using the inverse modeling capability of PHREEQC (Parkhurst and Appelo, 1999). Required input includes the initial and final water chemistry, along with uncertainty limits in the water analyses and allowed mineral-water phase reactions. Output includes modeled sets of possible reactions that can yield the observed differences between initial and final water composition. Inverse modeling was performed using Eagle 2 (WDNR average values) values as the initial water and Waukesha 9 as the final water. The uncertainty for each element in both analyses was set to ± 5% and the uncertainty in pH values was set to ± 0.1 units. Allowed reactions include precipitation/dissolution of calcite, dolomite, gypsum, pyrite, goethite, halite, and CO_2(gas). Two cation exchange sites were defined; (NaX and 0.6Ca:0.4Mg X_2). The 0.6Ca:0.4Mg X_2 exchange site is the stoichiometry of CEC sites found in Pewaukee 10 (see “aquifer solids” below). Cation exchange capacity (CEC) was set to the average found in Mount Simon sediments of Pewaukee 10 (see below) because most of the water produced from this well comes from the Mount Simon . Cation exchange reactions were allowed by assuming both exchange sites were originally at equilibrium with Waukesha 9 water. Both sites were allowed to re-equilibrate with incoming water from Eagle 2. Total mass transferred per liter of water for each mineral are given in Table 2. Negative values indicate mineral precipitation, positive values indicate dissolution.

Mineral	Moles transferred per liter
Calcite	-7.8E-4 (precipitated)
Dolomite	2.8E-4 (dissolved)
Gypsum	2.8E-3 (dissolved)
Pyrite	-8.5E-7 (precipitated)
Goethite	-1.2E-5 (precipitated)
Halite	1.8E-3 (dissolved)

Table 2: PHREEQC calculated mass transfers between Eagle 2 and Waukesha 9.

Results indicate the dedolomitization process precipitates ~0.8 millimoles of calcite per liter of water and that this is being driven by the dissolution of 2.8 millimoles of gypsum and ~0.3 millimoles of dolomite per liter of water. Cation exchange reactions contribute significantly to the water chemistry. Twenty seven percent of the observed Mg^{2+} increase and 5 percent of the observed Ca^{2+} increase along the flow path is due to cation exchange. Three percent of the Na^{+} that enters the system from dissolution of halite is ultimately sequestered on cation exchange sites. The PHREEQC modeling, both simple speciation and inverse modeling, gives a broad overview of the geochemical conditions in the aquifer, however care must be taken to avoid over interpretation. This is primarily due to the fact that the input data is obtained from average values over an interval of 34 years and the fact that aquifer solids have only been characterized in one well.

Aquifer solids

Relatively little information exists on the detailed mineralogy of the deep sandstone aquifer. A qualitative lithologic description of the entire stratigraphic section exists in eastern Sheboygan county, 87 km northeast of the study area (Moretti, 1971). A detailed analysis of the aquifer including quantitative petrology and mineralogy (Xray diffraction and thin section analysis) and cation exchange capacities with leachate analysis has been performed in Green Bay, 170 km north of the study area (CH2M-Hill, 2000). Both of these studies were performed on core samples obtained from exploratory wells. Because core samples do not exist within the study area itself, a detailed analysis

was performed on drill cuttings obtained from the newly drilled Pewaukee 10 well (see Figure 9). Although petrographic information is lost when using drill cuttings, primary mineralogic and cation exchange information is retained. Air was used as the circulating fluid to drill all but the last 70 meters (total depth is 402 meters). The last 70 meters were drilled with clear water as the fluid. No drilling additives or foreign liquids contacted aquifer solids during drilling.

Drill cuttings from ten intervals were subjected to thin section analysis (after epoxy impregnation), Xray diffraction analysis, cation exchange capacity (CEC) with leachate analysis, and extractable iron oxide content. CEC analyses were performed via standard sodium acetate extraction methods (Soil Soc. America, 1982). Amorphous iron oxides were extracted with ascorbic acid at pH 8 (Mettler, et al., 2001). Thin section analysis, quantitative mineralogy via X-ray diffraction and leachate analysis were performed commercially (Mineralogy, Inc., Tulsa, OK). Results of these analyses are given in Appendix A.

Drill cuttings representing all the major hydrostratigraphic units were collected. The uppermost unit within the aquifer (Sinnippee) is a clean dolomite. The remaining productive units (St. Peter, Wonewoc and Mt Simon) are remarkably clean quartz sandstones. The Eau Claire contains significant amounts of clay minerals and forms a leaky aquitard between the upper and lower sandstones. Shaley zones within the aquifer are dominated by an illite/smectite mixed layer clay that averages 75-80% illite. Traces of authigenic clay and iron oxide coatings are seen throughout. Mineralogically the aquifer is dominated by quartz and dolomite with lesser amounts of illite/smectite mixed layer clays. The same general mineralogy was reported from the Green Bay well (CH2M-Hill, 2000).

CECs reflect the dominant mineralogy. Quartz-rich samples average 1.9 meq/100g, dolomite-rich samples average 18.1 meq/100g and shaley zones average 24.1 meq/100g. Average CEC for the entire well is 9.9 meq/100g. This also is similar to the Green Bay well. Measured CEC values show that Ca^{2+} and Mg^{2+} constitute more than

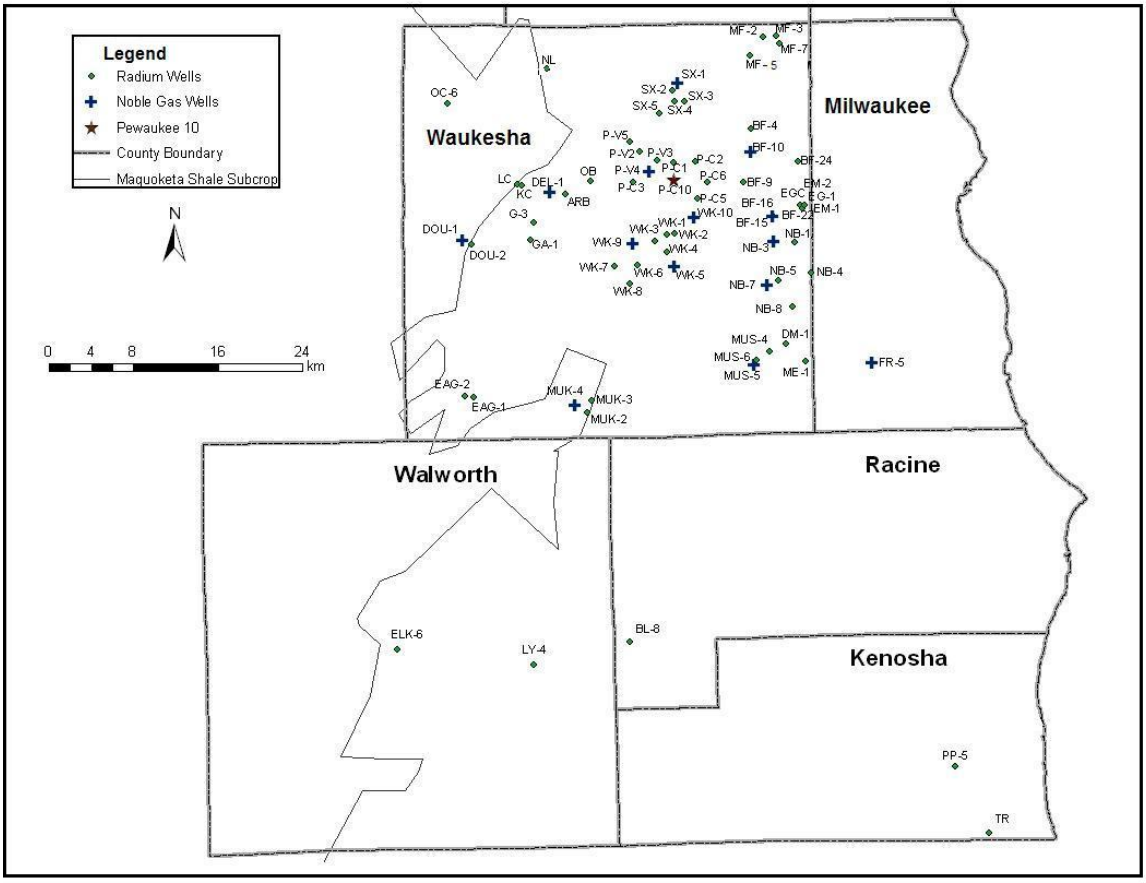

Figure 9: Location of wells used in this study. Three wells (Fort Atkinson 7, Jefferson 3, Johnson Creek 3) are located west of the primary study area in Jefferson County and are not depicted in this map.

79% of the total CEC. To determine if aquifer solids are close to equilibrium with aquifer water, PHREEQC surface complexation modelling was performed using water analyses from the well discharge along with average measured CEC for each element and the average ascorbic acid extractable iron. Average CEC values were used because there is no depth-discrete water quality information. All wells that intersect this aquifer are open throughout the entire stratigraphic interval.

In order to assign the moles of cation exchange sites available to a liter of aquifer water, aquifer porosity was chosen such that the calculated total CEC matched the

measured total CEC. The resultant value of 30% is a reasonable estimate for total porosity for sediments of this type and agrees with qualitative estimates based on the petrographic analysis of drill cuttings (Appendix A). Porosity measurements from core samples taken from the Green Bay well range from 17% to 28%.

PHREEQC calculated values generally agree with measured values for the primary exchanged ions, calcium and magnesium. Calculated values of exchanged calcium and magnesium are 120% and 54% of measured values respectively. Calculated values for Na^+ and K^+ do not match the measured values as well, probably due to the low levels of these ions on exchange sites and the increased relative importance of sampling error at these low concentrations.

The importance of divalent cation sorption to hydrous ferric oxide (HFO) surfaces with respect to CEC was also investigated during PHREEQC modelling. A HFO surface area of 600 m^2/g and a surface site density of 0.2 mole sites/mole HFO were assumed. These assumptions were used along with the average ascorbic acid extractable iron over the entire stratigraphic section of 1140 ppm. By far the largest pool for all divalent ions is on exchange sites, exceeding both the aqueous and the sorbed to HFO pools (Figure 10).

Radium Occurrence

Radium levels throughout eastern Wisconsin have been found to correlate with the edge of the Makoqueta subcrop (Grundl and Cape, 2006; Weaver and Bahr, 1991a). A similar correlation is also found in Illinois wells (Gilkeson and Cowart, 1982; Gilkeson, et al., 1978, 1983, 1984). Grundl and Cape (2006) found that the aquifer is everywhere at saturation with respect to barite and that co-precipitation of radium into barite served as a geochemical control on radium levels in the unconfined portion of the aquifer. As the aquifer transitions to confined conditions both radium and sulfate levels rise and barite co-precipitation ceases to control radium activities. An additional source of radium or an additional set of geochemical processes controls radium activities. Geochemical processes that can be invoked include co-precipitation into other sulfate

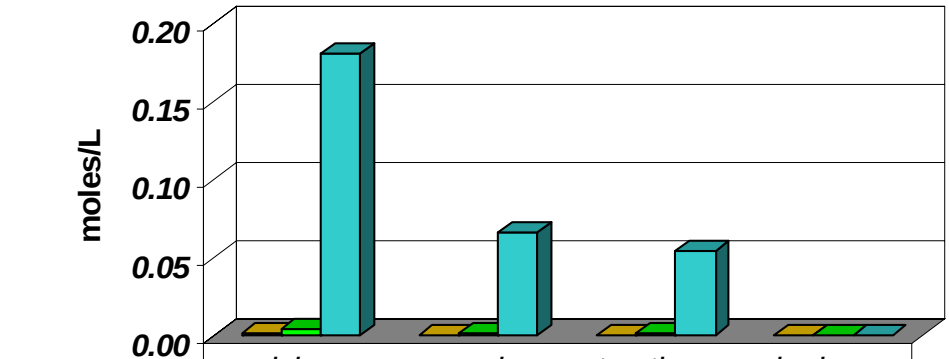

	calcium	magnesium	strontium	barium
aqueous	1.68E-03	9.67E-04	3.89E-04	2.70E-07
sorbed	3.81E-03	2.02E-03	1.42E-03	1.63E-06
exchanged	1.81E-01	6.64E-02	5.47E-02	3.40E-05

Figure 10: Relative importance of exchanged, sorbed and aqueous pools of divalent ions studied. Results are based on PHREEQC modeling as described in the text. Concentrations are given in terms of moles of ions encountered by a liter of aquifer water.

minerals, mobilization of colloids as a result of the influx of a dominantly univalent (HCO_3^-) recharge water into a dominantly divalent (SO_4^{2-}) water, or ion exchange reactions driven by the influx of less saline recharge water into the confined zone. Additional sources of radium in the confined portion may include shaley zones within the aquifer that are being subjected to large vertical heads as a result of large scale pumpage or deep seated brines originating from the Michigan Basin that still remain in the deepest portions of the aquifer that have not been actively flushed. Each of these possibilities was investigated as a part of this research.

Co-precipitation into sulfate minerals

Theoretical considerations show that sulfate minerals readily accommodate radium into their lattice structure whereas carbonate minerals do not (Langmuir and Riese, 1985; Zhu, 2004). The principal indicators that radium is controlled by the sulfate mineral barite ($BaSO_4$) in the unconfined portion of the aquifer are a) saturation with

respect to barite and b) a constant Ra:Ba atom ratio in the water in spite of variability in the absolute concentrations of both ions (Grundl and Cape, 2006). Both radium isotopes exhibit constant Ba:Ra ratios. In the confined zone, SO_4^{2-} concentration and radium activities both increase causing Ra:Ba ratios to sequentially rise as barite solubility forces the corresponding Ba^{2+} concentrations to very low levels. The highly insoluble barite cannot control radium in the presence of high levels of sulfate.

Twenty eight individual wells within Waukesha county have been measured at one time or another for Sr^{2+} concentrations and these wells indicate that the confined portion of the aquifer is also at saturation with respect to celestite ($SrSO_4$) whereas unconfined wells are undersaturated. Most of these strontium analyses were performed at different times from the rest of the major ions therefore in order to make solubility calculations it was assumed that major ion chemistry does not change over time – an assumption that is supported by previous findings (Schmidt, 2002). Six wells were found that were sampled at one time for barium, radium, strontium and the major ions (the entire New Berlin well field). All six of these wells are in the confined portion of the aquifer and are at saturation with respect to both celestite (SI = -0.20 ± 0.08) and barite (SI = -0.08 ± 0.08). These six wells exhibit constant Ra:Sr atom ratios for both radium isotopes (^{226}Ra:Sr = 4.3 (±1.8)x10^{-11} (standard deviation) and ^{228}Ra:Sr = 1.9 (±0.7)x10^{13}). Thus, the same two indicators (saturation and constant Ra:Sr ratio) suggest that radium activities in the confined portion of the aquifer are controlled by co-precipitation into the sulfate mineral celestite in the same manner as barite control in the unconfined aquifer.

The conceptual model is that of an aquifer preferentially flushed in the unconfined portion leaving only the very insoluble barite ($K_{sp} = 10^{-9.96}$) behind. The confined portion of the aquifer is poorly flushed and still contains the more soluble minerals gypsum and celestite. Gypsum ($K_{sp} = 10^{-4.59}$; 2.3x10^5 times more soluble than barite) is actively dissolving whereas celestite ($K_{sp} = 10^{-6.67}$; 2x10^3 times more soluble than barite) has reached saturation. Active gypsum dissolution provides sulfate concentrations of 100 to 300 ppm. At this sulfate concentration, celestite at saturation provides ~30 to 17 ppm

Sr^{2+}. Radium ions are able to co-precipitate into the celestite lattice as Sr^{2+} continually dissolves and precipitates across the saturated mineral-water interface. Barite, which is also at saturation in the confined portion of the aquifer, also has continual dissolution and precipitation across its saturated mineral-water interface, but can only supply parts per billion levels of Ba^{2+} hence very little radium is co-precipitated. Effective control of radium activities shifts from barite in the unconfined aquifer to celestite in the confined aquifer. Equation 1 can be written to predict the level of radium activity possible according to this model of sulfate mineral co-precipitation.

$$Ra_{tot} = {}^{226}Ra + {}^{228}Ra$$

$$Ra_{tot} = \{[({}^{226}X_{Ba})(Ba^{2+}) + ({}^{226}X_{Sr})(Sr^{2+})]*[(N)(\lambda_{226})/2.2]\} + \{[({}^{228}X_{Ba})(Ba^{2+}) + ({}^{228}X_{Sr})(Sr^{2+})]*[(N)(\lambda_{228})/2.2]\} \quad \text{Eqn. 1}$$

Where:

Ra_{tot} = total radium activity

${}^{226}Ra$ = ${}^{226}Ra$ activity

${}^{228}Ra$ = ${}^{228}Ra$ activity

X_{Ba} = the Ra:Ba molar ratio for each isotope

X_{Sr} = the Ra:Sr molar ratio for each isotope

Ba^{2+}, Sr^{2+} = Molar concentration of each element

λ = decay constant (min^{-1})

N = Avagadro's number

Figure 11 is a comparison of radium activities as predicted from Equation 1 and the corresponding measured activities for all wells in the study area for which strontium data exists. The molar ratios ${}^{226}X_{Ba}$ and ${}^{228}X_{Ba}$ ($1.2\ (\pm 0.8)\times 10^{-8}$ and $4.3\ (\pm 2.9)\times 10^{-11}$, respectively) were taken from Grundl and Cape (2006). The molar ratios ${}^{226}X_{Sr}$ and ${}^{228}X_{Sr}$ ($4.3\ (\pm 1.8)\times 10^{-11}$ and $1.9\ (\pm 0.7)\times 10^{-13}$) are the average of the ratios observed in the six New Berlin wells that have coincidental major ion and strontium data (the six rightmost data points in Figure 11 plots). The average difference between predicted and measured

combined radium activity is 3.2 pCi/L. The average difference between predicted and measured activities of ^{226}Ra and ^{228}Ra are 1.4 and 2.2 pCi/L respectively. The large mismatch observed in the Timber Ridge well is unexplained. One possibility is that the single radium measurement available for this well is anomalously high (23.9 pCi/L total Ra) and may be in error. Three wells are not included in Figure 11; Elkhorn 6, Lyons 4 and Eagle 2. Sulfate levels in these wells (< 5 ppm) are too low to allow accurate prediction.

A rigorous analysis of error is difficult to make for this simple predictive model. Error bars on predicted values of ^{226}Ra and ^{228}Ra are based on the standard deviations of the X_{Ba} and X_{Sr} molar ratios. Equation 1 was solved using plus one standard deviation and minus one standard deviation for both X_{Ba} and X_{Sr} and the resultant values were used as endpoints for the error bars.

The amount of radium contained in either barite or celestite can be estimated from the molar ratios observed in the water in combination with published partition coefficients between both minerals and water. Zhu (2004) reports distribution coefficients between water and barite as well as water and celestite for several trace elements including radium. Radium is the most highly partitioned element with Kd values of 1.5 and 228 for barite and celestite respectively. Partitioning is a slight function of mineral composition and these values are for 1% radium content. Langmuir and Riese (1985) report Kd values of 1.8 and 280 respectively. Using these partition coefficients, the concentration of radium is between 18 and 21 ppb in barite and between 12 and 15 ppb in celestite.

Mobilization on colloidal particles

It is possible to transport radium, or the parent isotopes, on colloidal sized particles either as a part of the colloidal mineral itself or sorbed to the surface of the particle. In this aquifer system, colloids can be released as the flow of relatively fresh, HCO_3^- water replaces more saline and sulfate-rich water beneath the Maquoketa shale.

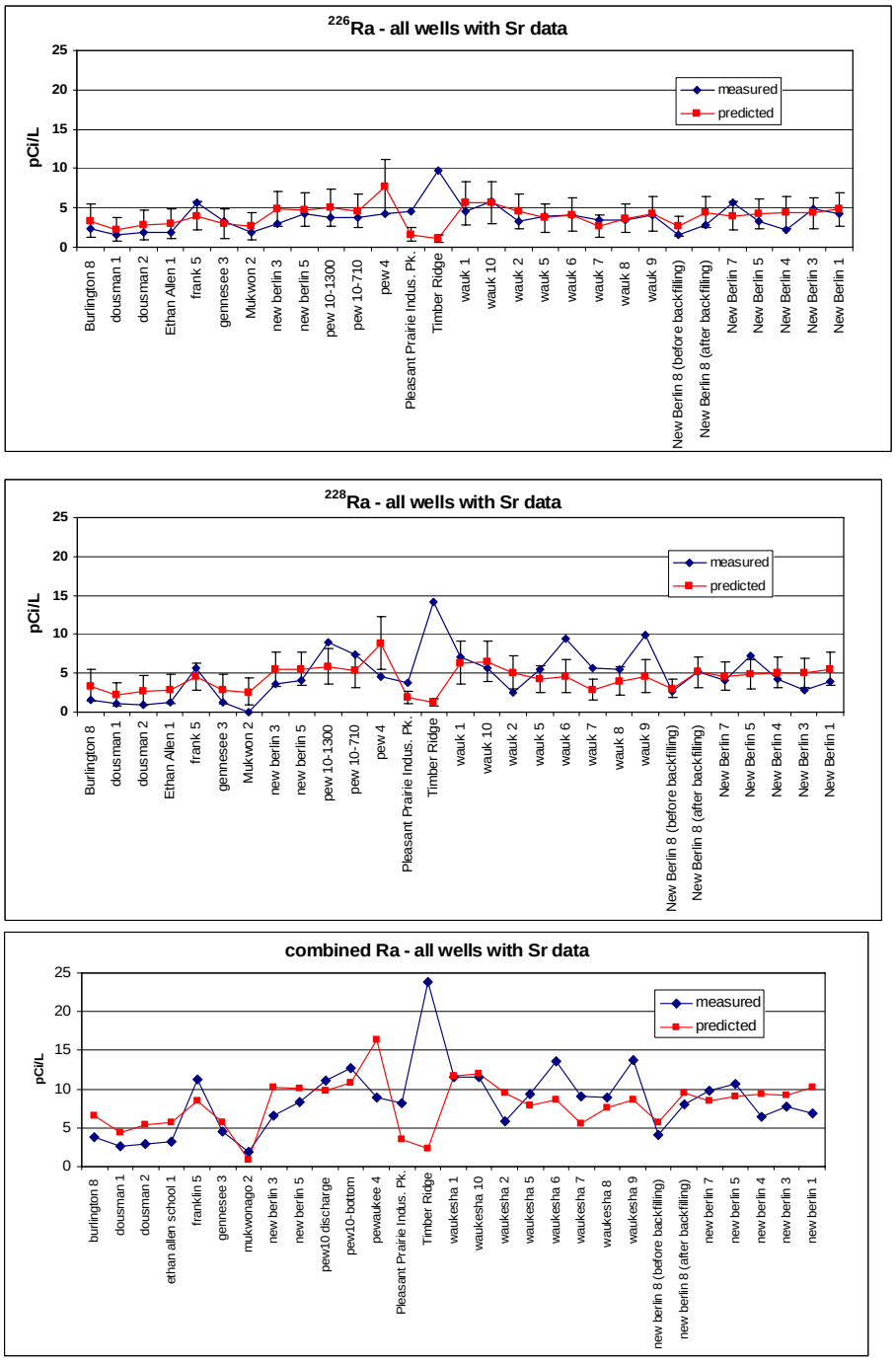

Figure 11: Match between predicted and measured radium levels in all wells with strontium data. The six rightmost New Berlin wells were used to establish the Ra^{2+}/Sr^{2+} ratio for use in Equation 1. Significance of error bars discussed in the text.

Well Name	WDNR id number	^{226}Ra (pCi/L)	^{228}Ra (pCi/L)	combined Ra (pCi/L)	Ba^{2+} (mg/L)	Sr^{2+} (mg/L)	predicted ^{226}Ra (pCi/L)	predicted ^{228}Ra (pCi/L)	predicted Ra comb (pCi/L)
Burlington 8	bg737	2.3	1.5	3.8	0.14	5.5	3.3	3.3	6.6
Dousman 1	bh392	1.6	1.1	2.7	0.11	0.97	2.3	2.1	4.4
Dousman 2	bh393	1.9	1.0	2.9	0.139	0.61	2.8	2.6	5.4
Eagle 2	bh395	1	3	4	0.86	1.1	16.9	15.9	32.8
Elkhorn 6	bh179	7.9	1.7	9.6	0.75	0.48	14.7	13.8	28.5
Franklin 5	bg451	5.6	5.6	11.2	0.021	32	4.0	4.6	8.6
Genessee 3	bh359	3.3	1.2	4.5	0.13	3.4	2.9	2.8	5.7
Genessee 3	bh359	1.9	1.3	3.2	0.13	3.4	2.9	2.8	5.7
Lyons 4	bd130	4.5	4.4	8.9	1.6	1.6	31.5	29.5	61.0
Mukwon 2	bh406	1.9	0	1.9	0.13	1.3	2.7	2.6	5.2
New Berlin 3	bh411	3	3.6	6.6	0.035	37	4.8	5.5	10.3
New Berlin 5	bh413	4.2	4.1	8.3	0.027	38	4.8	5.5	10.3
New Berlin 8 before backfilling	bh416	1.5	2.6	4.1	0.023	20	2.7	3.0	5.7
Pewaukee 10-1300	--	3.7	9	12.7	0.037	39	5.1	5.8	10.9
Pewaukee 10-710	--	3.7	7.4	11.1	0.037	35	4.6	5.3	9.9
Pewaukee 4	bh423	4.3	4.6	8.9	0.038	62	7.7	8.8	16.5
Pleasant Prairie Indus. Pk.	bg085	4.5	3.7	8.2	0.021	11	1.6	1.8	3.5
Timber Ridge	bg086	9.7	14.2	23.9	0.011	7.7	1.1	1.2	2.3
Waukesha 1	bh427	4.5	7.1	11.6	0.076	37	5.6	6.3	11.9
Waukesha 10	bh436	5.8	5.7	11.5	0.04	43.63	5.6	6.5	12.1
Waukesha 2	eq944	3.3	2.5	5.8	0.057	30.67	4.5	5.1	9.6
Waukesha 5	bh431	3.9	5.5	9.4	0.042	26.11	3.7	4.2	7.9
Waukesha 5	bh431	3.1	6	9.1	0.042	19	2.9	3.3	6.2
Waukesha 6	bh432	4.1	9.5	13.6	0.071	24.64	4.1	4.5	8.7
Waukesha 7	bh433	3.4	5.6	9	0.055	14.17	2.7	2.9	5.5
Waukesha 8	bh434	3.4	5.5	8.9	0.056	22.55	3.6	4.0	7.6
Waukesha 9	bh435	4.1	9.9	14	0.046	20.19	3.1	3.5	6.6
Waukesha 9	bh435	4.1	9.9	14	0.089	22	4.2	4.5	8.7
Calibration analyses									
New Berlin 8 after backfilling	bh416	2.9	5.2	8.1	0.022	36	4.4	5.1	9.6
New Berlin 7	bh415	5.7	4.1	9.8	0.022	32	4.0	4.6	8.6
New Berlin 5	bh413	3.3	7.3	10.6	0.022	34	4.2	4.9	9.1
New Berlin 4	bh412	2.2	4.3	6.5	0.019	36	4.4	5.1	9.5
New Berlin 3	bh411	4.9	2.8	7.7	0.023	35	4.4	5.0	9.4
New Berlin 1	bh409	2.9	4.26	7.16	0.023	39	4.8	5.5	10.3

Table 3: Measured and predicted radium values for wells in SE Wisconsin. Multiple entries for the same well indicates different analyses from the same well. Calibration analyses were used to generate X_{Sr} in Equation 1. Pewaukee 10 values are from depth discrete samples taken at 710 ft bgs (representative of overall well discharge) and 1300 ft bgs (within 20 ft of the bottom).

This process is being greatly enhanced by the large scale withdrawals from this aquifer (cf. Figure 4). Previous studies have shown that a change in pH, in salinity or in the valence of the primary anion are sufficient to release colloidal particles to the groundwater (Grolimund, et al., 2001; Bunn, et al., 2002).

To test for this possibility the Waukesha 6 and Waukesha 10 wells were selected for ultrafiltration and analysis of the resultant colloidal particles. These wells were selected because they are located within 8 km of each other, are drilled to essentially the same depth (2075 feet and 2145 feet respectively), have similar major ion chemistry, and there is a long history of radium analyses that indicates a high and relatively constant radium activity and $^{226}Ra/^{228}Ra$ isotope ratio for each well since at least 1982. During this period of time Waukesha 6 averaged 13.6 (±2.5) pCi/L and Waukesha 10 averaged 11.5 (±1.8) pCi/L total radium. The two wells do exhibit different isotope ratios. ^{228}Ra dominates in Waukesha 6 (^{226}Ra = 4.1 pCi/L; ^{228}Ra = 9.5 pCi/L) whereas Waukesha 10 has equal activities of both isotopes (^{226}Ra = 5.8 pCi/L; ^{228}Ra = 5.7 pCi/L) Most high radium wells in southeast Wisconsin exhibit isotope ratios similar to that of Waukesha 6.

Samples were collected on consecutive days from both wells and transported to the laboratory for ultrafiltration in an anaerobic chamber. In order to avoid the possible oxidative precipitation of ferric oxides, care was taken to minimize contact with the atmosphere during both sampling and analysis. Sample bottles were flushed with nitrogen gas prior to sampling. During sampling nitrogen gas was bubbled through the water until the bottle was sealed (no headspace). Two separate filtration steps were performed using 0.45μm and 10,000 Daltons (approximately 0.025μm) filter paper. The colloidal size fraction was obtained from the difference between the two filtration steps. All filtering was done within the anaerobic chamber. This experimental design is based on an operational definition of colloidal particles as being between 0.45um and 10,000 Daltons in size. Raw water as well as filtrate and the filter paper from each step were analyzed for radium activity. Additional aliquots were collected for major ion analysis. All radium and

ionic analyses were performed by the State Lab of Hygiene. Wells were purged for a minimum of 7 hours to assure that native groundwater was being collected. Results for the filtered water and the filtrant remaining on the filter paper are given in Table 4. The experimental data indicate that essentially none of the radium activity is being carried on particulate matter, either coarse grained (>0.45μm) or colloidal (difference between 0.45μm and 10K Dalton). Colloidal transport of radium activity appears to be unimportant in this aquifer.

In order to ascertain the gross mineralogy of the particulate matter, filtrant was acid digested and analyzed by ICP atomic emission spectroscopy for total aluminum, barium, calcium, iron, magnesium, potassium, and sodium. Comparison of weight ratios of these elements gives an idea as to the probable mineralogy of the particulates. The very low Al:Fe ratios in both size fractions indicates the presence of ferric oxide minerals with few aluminosilicate minerals (ie. clays). Among clay minerals, illite exhibits an Al:K ratio of 1:5 and smectite clays contain no K (Al:K ratio ~ ∞), therefore the Al:K ratios of 7.99 and 3.12 in the colloidal fraction indicate that the few aluminosilicate minerals that are present are mixed layer illite/smectite. This is in agreement with the mineralogy of clay minerals seen in Pewaukee well 10. There is also a large calcite/dolomite component as indicated by the high absolute amounts of calcium and magnesium. To the extent that these measurements are representative of the aquifer as a whole, the geochemical reactivity of colloids in this aquifer will be dominated by reactions with ferric oxide minerals; carbonate minerals are much less reactive and few clay minerals are present.

Possible additional sources of radium

It is possible that radium resides preferentially in brines originating from the Michigan Basin that still remain in the deepest portions of the aquifer that have not been actively flushed. Testing this hypothesis is problematic because all deep sandstone wells in southeast Wisconsin are open from the base of the Maquoketa shale to the bottom of the well. There are no vertically discrete water quality data available. In spite of this,

conventional wisdom holds that radium is found preferentially in the deepest water and as a result, three wells within the county (Waukesha 2, Waukesha 7 and Waukesha 9) have been backfilled in an attempt to reduce the radium levels produced by each well. Reductions in radium levels as a result of this rather drastic procedure are mixed. Radium levels before and after backfilling are shown in Table 5. Waukesha 2 and 7 show a moderate decrease in radium activity whereas Waukesha 9 shows an increase although only one measurement has been made in this well after backfilling. It is clear that well capacity has been significantly reduced by the loss of several hundred feet of productive aquifer.

When radium activities from Waukesha county wells are plotted against the thickness of the Mount Simon formation within each well, a subtle relationship appears for ^{228}Ra (Figure 12). Although visually subtle, this relationship has a Spearman rank coefficient of 0.66 which means that the relation is statistically valid at a 99% confidence level. No equivalent relationship is seen for ^{226}Ra (Figure 12). The difference in behavior between ^{228}Ra and ^{226}Ra may be due to the fact that the ^{226}Ra decay chain contains uranium isotopes whereas the ^{228}Ra decay chain contains only thorium. Uranium is mobile in groundwater systems and variations with depth in the concentration of the uranium parent would be smoothed out by this mobility. Thorium is essentially immobile thus preserving the record of any depth variations in the daughter isotope ^{228}Ra. This also may be the reason for the relative constancy of ^{226}Ra activities in the aquifer as a whole when compared to the more variable ^{228}Ra activity.

Radium activities shown in Figure 12 are averages of all measurements taken since 1982. Not all wells have the same number of measurements. The Mount Simon formation was used for comparison because it is the deepest, as well as the most productive, formation within the aquifer and as such is a direct measure of the amount of deep water produces from a given well. Any increase in radium activity with depth is subtle at best. It should be noted that highly radioactive water has been found at depth in a deep well drilled 70 km to the southeast along the shore of Lake Michigan (99 pCi/L at 3120 feet below ground surface) (Nicholas, et al., 1984).

Because of the complete lack of vertically discrete data, a series of nine wells were sampled in a vertically discrete manner. All nine wells were municipal wells that were being repaired and had a small sampling pump (500 to 1000 gpm) installed. Samples were collected with the sampling pump on by lowering a thief sampler through a tremie pipe to a predetermined depth. Because the well was actively pumped, each succeeding sample represented a mix of water entering the well from the ever longer open section below. For four of these wells, sampling was done in conjunction with flow meter logging in order to ascertain the volume of flow entering the well at each interval. Flowmeter logging was performed by WGNHS personnel (Ken Bradbury and Dave Hart, personal communication). Mixed concentrations measured at each interval, in combination with the logged percentage of flow entering the well at each interval, were used to ascertain the un-mixed composition at each sample depth. Unfortunately, the flow meters were insufficiently accurate to rectify the flow entering these large diameter municipal wells and un-mixing calculations were not possible.

The effect of cation exchange reactions was investigated by simple advective flow modeling within PHREEQC. The flow between Eagle 2 (upgradient well) and New Berlin 8 (downgradient well) was represented by a 40-cell column. Twenty pore volumes of water were advected through the column and cation exchange reactions were allowed to reach equilibrium. The cation exchange capacity was set to the average value measured in Pewaukee 10 for the Mount Simon formation (6.2 meq/100g). Only the Mount Simon was used because flowmeter data indicate ~94% of the total groundwater flow is transmitted through this formation in this part of the aquifer (Ken Bradbury and Dave Hart, personal communication). Exchange constants for the major ions were taken from the WATEQF4 database. The radium exchange constant was taken from Tachi, et al. (2001). Solids were first equilibrated with New Berlin 8 water followed by flushing with Eagle 2 water. Modeled radium activities were tracked at the outlet of the column. Both upgradient and downgradient waters are Ca^{2+} and Mg^{2+} dominated although upgradient (influent) water is more dilute causing a net loss of ions from the water at the advective front (1 pore volume). After ~5 pore volumes, cation exchange reactions reach

	Raw water		0.45 μm water		10,000 Dalton water		0.45 μm filtrant		10K Dalton filtrant	
	^{226}Ra	^{228}Ra	^{226}Ra	^{228}Ra	^{226}Ra	^{228}Ra	^{226}Ra	^{228}Ra	^{226}Ra	^{228}Ra
Waukesha 6	3.8 (±0.4)	9.0 (±1.1)	3.4 (±0.3)	11 (±1.0)	3.3 (±0.4)	10 (±1.0)	0.01 (±.07)	0.2 (±0.3)	0.17 (±0.07)	0.2 (±0.3)
Waukesha 10	6.4 (±0.4)	3.4 (±0.8)	5.4 (±0.4)	4.0 (±0.8)	5.6 (±0.4)	4.5 (±0.8)	0.46 (±0.09)	0.5 (±0.3)	0.27 (±0.07)	0.2(±0.3)

	Al	Ba	Ca	Fe	Mg	K	Na	Al:Fe	Al:K
	μg per liter of water filtered							weight ratio	weight ratio
Waukesha 6									
0.45μm filtrant	37	6	1129	2713	183	99	124	0.03	0.29
10K Dalton filtrant	220	15	1724	5708	2670	122	445	0.08	1.81
colloidal fraction	184	10	595	2995	2487	23	321	-0.06	7.99
Waukesha 10									
0.45μm filtrant	20	1	652	672	153	69	175	0.01	0.37
10K Dalton filtrant	238	7	2060	1552	247	139	353	0.15	1.71
colloidal fraction	218	6	1408	880	94	70	178	0.25	3.12

Table 4: Results of colloids analysis. Radium values are in pCi/L. ± values represent the standard deviation as obtained from counting statistics. Colloidal fraction is obtained by subtracting the mass of filtrant collected on the 10K Dalton filter from the mass collected on the 0.45 μm filter. This analysis was done only once hence no estimate of error is reported.

	Mt Simon thickness (ft)	amount of backfill (ft)	^{226}Ra (pCi/L)	^{228}Ra (pCi/L)	Ra_{tot} (pCi/L)
Waukesha 2	715	125			
before backfill			3.1(±0.4)	3.3(±0.4)	6.4(±0.6)
after backfill			3.3(±0.1)	2.5(±0.2)	5.8(±0.3)
Waukesha 7	1026	491			
before backfill			3.7(±1.8)	6.2(±0.2)	9.9(±2.2)
after backfill			2.3(±0.2)	3.9(±0.9)	6.2(±0.9)
Waukesha 9	1306	501			
before backfill			4.0(±0.3)	9.7(±2.0)	13.7(± 2.0)
after backfill			5.1	12	17.1

Table 5: Radium activities before and after backfilling of three Waukesha county wells. Error values are ± one standard deviation of all measurements since 1982. Not all wells have the same number of measurements. Only one measurement has been made in Waukesha 9 after backfilling.

completion and an 8% rise in radium activity along with small increases in calcium and magnesium were observed in conjunction with a decrease in sodium. No peak of radium was detected at any point. It seems unlikely that cation exchange reactions cause significant increases in radium activities in the downgradient, confined portion of the aquifer.

Geochemical tracer study

The confined aquifer of southern Wisconsin near Lake Michigan shows water moving slowly and continuously eastward at least since the last episode of Pleistocene glaciation (Feinstein, et al., 2005). The geochemical evolution from a Ca-HCO_3 character in the recharge area to a Ca-SO_4 character downgradient, increasing salinity and dedolomitization reactions eastward along the flow path are all in agreement with flow modeling results. A study using noble gas and stable isotopic tracers was undertaken to further understand aquifer conditions in the confined portion of the aquifer.

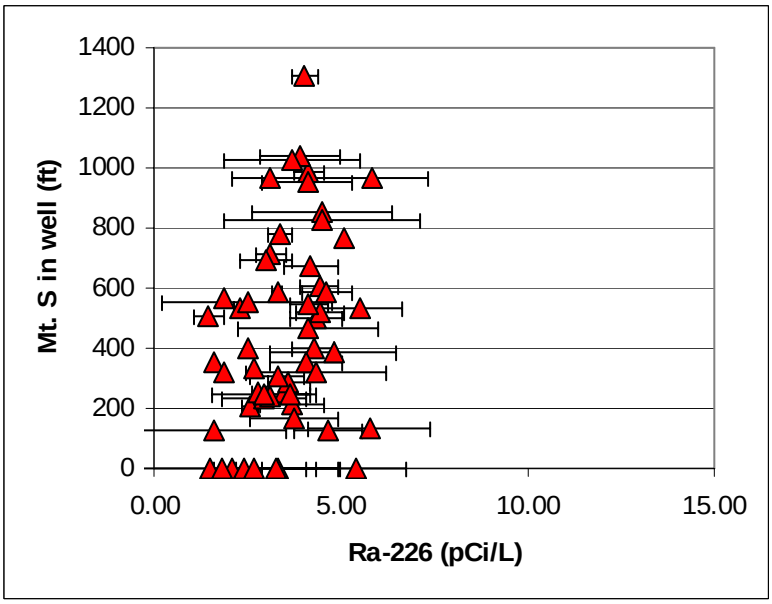

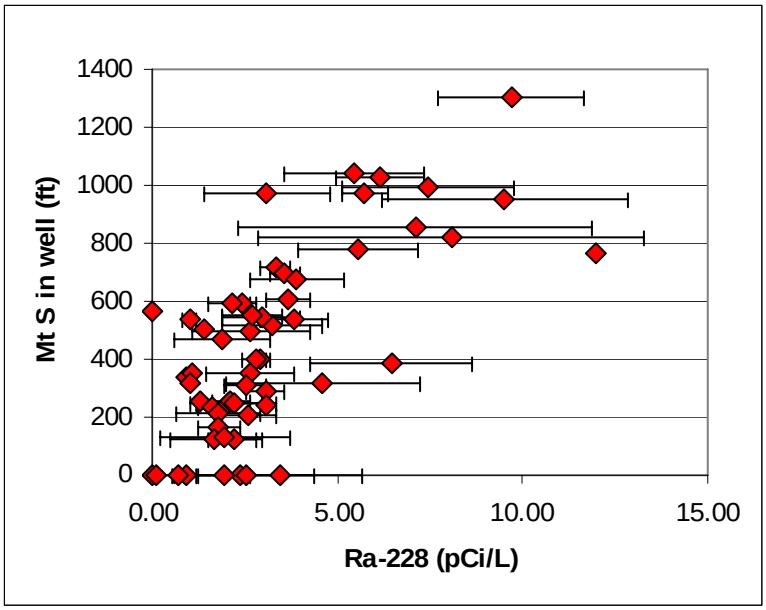

Figure 12: Radium activities versus total amount of Mount Simon formation in the wells of Waukesha county. Error bars are ± one standard deviation of all measurements since 1982. Not all wells have the same number of measurements.

Fifteen wells were selected for noble gas and stable isotope analysis (see Figure 9). Noble gas samples were collected from the wellhead spigot through clear plastic tubing into ~1 meter long section of 0.7 cm diameter copper tubing. The ends of the copper tubing were sealed by crimping. Clear plastic tubing was used to insure that no entrained bubbles were present. All wells were pumped for at least 15 minutes before sampling. Samples were shipped to the Swiss Federal Institute of Technology in Zurich Switzerland for analysis by mass spectrometry after cryogenic separation (Beyerle, et al., 2000). Stable isotope samples were collected at the same time and placed in 125 mL plastic bottles with no headspace. Samples were shipped to the University of Bern for analysis by mass spectrometry.

Noble gas geothermometry and stable isotopic data reveal a pulse of water at 15 km downgradient that was recharged at ~1^{o}C, well below the average annual temperature in this region today (Figure 13). Similar trends in noble gas temperatures have been reported in southern Michigan (Ma et al., 2004). This pulse of cold recharge is presumed to have occurred during the last glacial event when climatic conditions were much colder (e.g. Perry et al., 1982; Gilkeson et al., 1984). Average flow rates derived from groundwater flow modeling (Feinstein et al., 2004) and the presence of cold recharge water in the aquifer both suggest that waters in the confined aquifer are Pleistocene in age. Noble gas and stable isotope data are given in Appendix C.

The phenomenon of excess air refers to the universally noted fact that groundwaters contain more dissolved noble gases than would be predicted from local atmospheric pressure and temperature conditions. Extra air is injected into groundwater as small bubbles of soil gas get trapped as the groundwater rises during a recharge event. The amount of excess air found in a given groundwater is a direct function of the pressure differential developed during recharge and an inverse function of soil temperature. If the recharge dynamics of a given system remain constant over time, the amount of excess air can be used to deduce changes in soil temperature (ie. climate change). The reader is referred to Kipfer (2002) for a detailed description of the process of excess air generation.

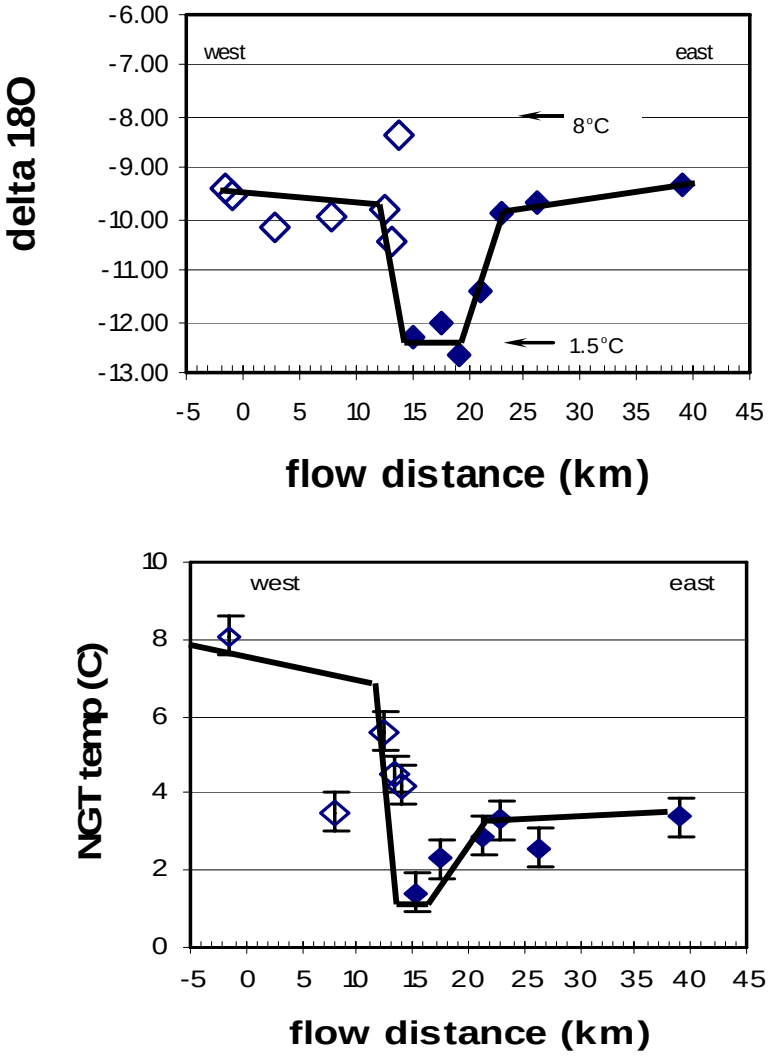

Figure 13: $\delta^{18}O$ and noble gas temperature (NGT) trends along an east-west transect from recharge area (0 km). Reference temperatures on $\delta^{18}O$ plot are from the worldwide average equation of Dansgaard (1964). Noble gas temperatures are calculated using the closed system equilibration model (Kipfer et al., 2002). Waters younger than Pleistocene glacial recharge are shown with open symbols.

The amount of excess air dissolved in Waukesha county groundwater begins to rise abruptly in the same wells that exhibit the pulse of cold recharge seen in Figure 13. This increase does not follow the temperature-solubility relation seen in younger waters (Figure

14). This abrupt change in excess air signifies an equally abrupt change in the recharge dynamics. This could be ascribed to a large increase in the average annual recharge event which seems unlikely as it would necessitate a drastic change in the annual precipitation. A more likely source is recharge by glacial meltwater, which contains abundant excess air. The conceptual model is diagrammed in Figure 15. Downgradient wells with older water reflect a time at which permafrost sealed the aquifer from the atmosphere and recharge was directly from glacial meltwater. The excess air signal is not high enough to suggest meltwater was derived solely from basal melting; a portion had to originate as percolating surface meltwater. This requires a fully saturated aquifer in order to avoid re-equilibration with soil gas in the vadose zone. A glacier with a frozen ice margin and a fully saturated aquifer has been proposed for the southern Laurentide ice sheet (Cutler *et al.,* 2000a; Winguth *et al*., 2004). Younger, upgradient wells were recharged by normal precipitation events as are seen today. The amount of excess air in these wells is a reflection of climatic warming since the retreat of the last Pleistocene ice cover. The sudden change to a temperature controlled excess air signal is due to the sudden change from glacial to precipitation based recharge as the permafrost seal finally broke and the ice began to retreat.

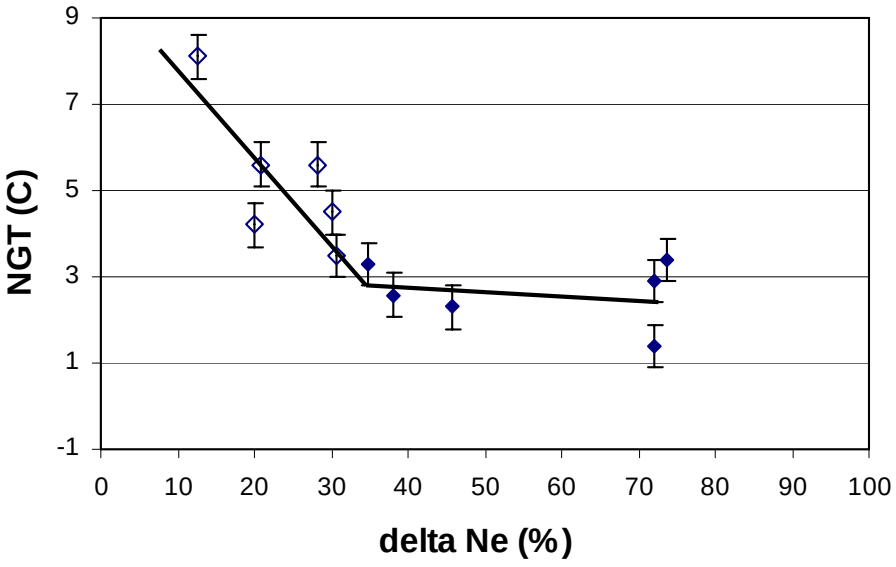

Figure 14: Percent excess air signal (plotted as percent excess Ne) versus noble gas temperature. Noble gas temperatures calculated using the closed system equilibration model (Kipfer et al., 2002). Waters younger than Pleistocene glacial recharge are shown with open symbols.

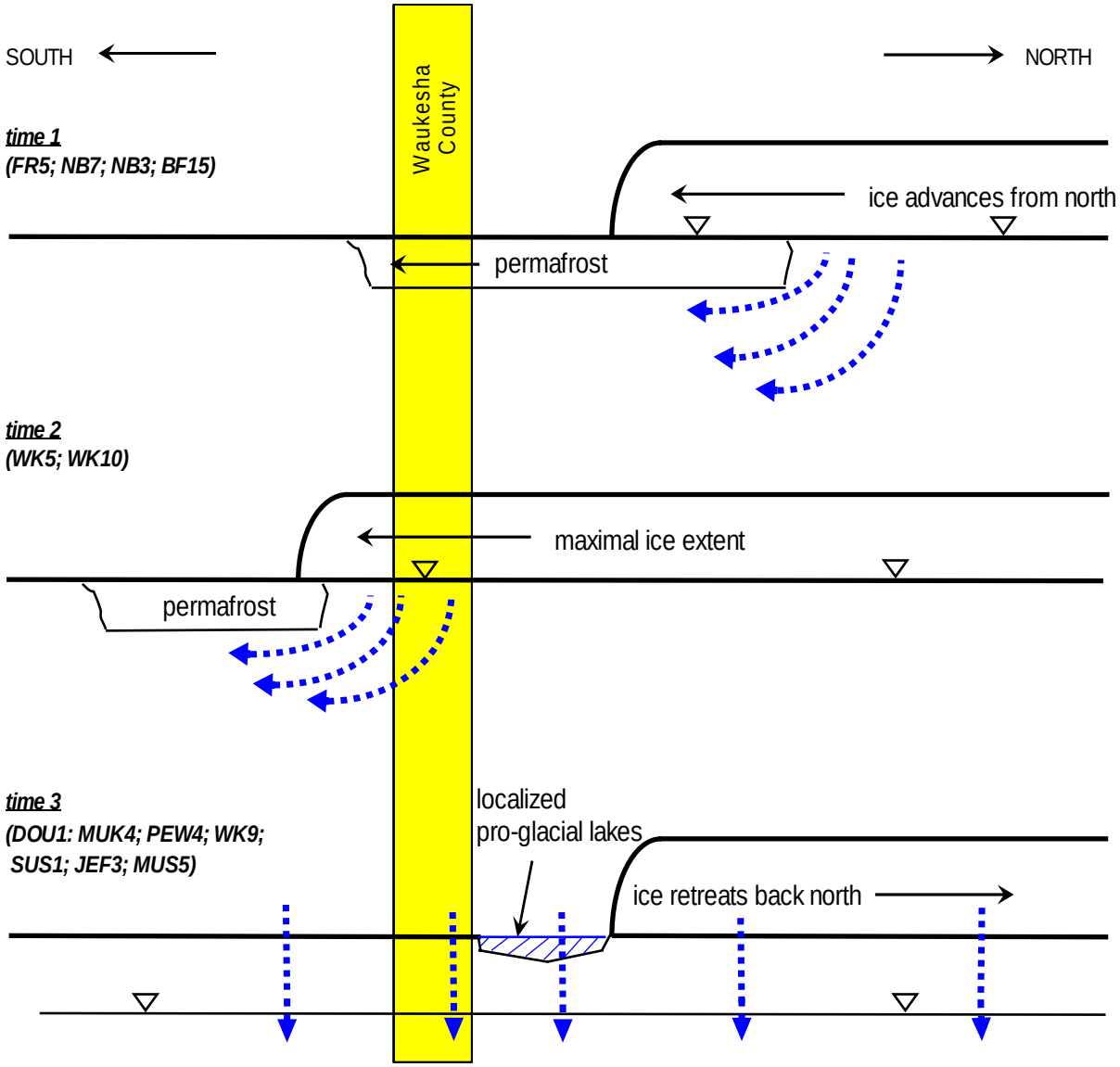

Figure 15: Diagrammatic north-south transect showing the proposed recharge sequence seen in the wells of Waukesha and Milwaukee counties. Initially (time 1) permafrost seals the fully-saturated aquifer and it is recharged by glacial meltwater. This occurs as the ice sheet advances into the area. Climate warming occurring during the maximal ice extent gradually thins the permafrost seal (time 2) until it eventually breaks and aquifer recharge becomes precipitation based (time 3). Dashed (blue) arrows indicate water movement. Well names for each time step are indicated.

Conclusions

The primary goal of this project was to determine the causes behind high radium activities in the Cambro-Ordovician aquifer in Waukesha county and southeast Wisconsin in general. This necessitated the collection and interpretation of a wide range of physical and geochemical data in order to gain a clear understanding of the physical and chemical dynamics of the aquifer. The overall interplay between the physical flow pattern and the chemical dynamics of this vitally important water resource has been elucidated. Defining this interplay is one of the novel aspects of this study and this has lead to the identification of which geochemical processes control radium levels in this aquifer system and which do not.

The conceptual model that emerges is that of an aquifer preferentially flushed by localized flow cells in the unconfined portion (west of the Maquoketa subcrop). Confined flow east of the subcrop is much slower and moves uniformly to the east. This has been in effect since the retreat of the last glacial ice cover. The ultimate source of radium is unclear although it may originate from source rocks within the aquifer itself. Regardless of source, the geochemical process that apparently controls radium levels in the aquifer is co-precipitation into sulfate minerals. In the actively flushed, unconfined portion of the aquifer the only sulfate mineral at saturation is the very insoluble barite. Co-precipitation into barite holds radium activities to below the federally mandated level of 5 pCi/L total radium. In the poorly flushed, confined portion, celestite is found at saturation and co-precipitation control shifts to this mineral phase. Celestite is more soluble and radium levels can rise above the mandated limit. Other geochemical processes such as cation exchange and colloidal transport do not appear to contribute to the high radium levels seen in the confined parts of the aquifer.

Specific advances that resulted from this work include:

1) The compilation of major ion, radium and stratigraphic data for wells in the study area. This data was used to identify and quantify the classic dedolomitization pattern of geochemical evolution of the aquifer along the flow path. This provides workers

with a geochemical backdrop against which future contamination questions can be assessed.

2) The collection of much needed information on the mineralogy and cation exchange capacity of aquifer solids in the area. Knowledge of aquifer solids is vital to geochemical modeling of the aquifer. Previously, this information was entirely lacking.
3) The use of detailed numerical flow modeling to define the flow patterns in the present day aquifer. Stable isotope and noble gas analyses were used to deduce the fact that Pleistocene age water is being pumped from eastern Waukesha and Milwaukee counties and that this water is likely to have originated directly from glacial meltwater.
4) The determination that radium activities in the aquifer are controlled by co-precipitation into sulfate minerals. Barite is the controlling mineral in the more actively flushed, unconfined portion of the aquifer that lies to the west of the Makoqueta subcrop. Celestite is the controlling mineral in the poorly flushed confined portions of the aquifer. Apparent concentration of radium in these two mineral phases is between 12 and 21 ppb.
5) An investigation into the possibility that radium is found preferentially in the deeper portions of the aquifer. This effort was hampered by a paucity of vertically discrete chemical data that precludes a definitive answer to this question. Comparison of radium activity versus length of screen in the lowermost Mt. Simon formation provides subtle evidence that ^{228}Ra may be preferentially found in the deeper aquifer however radium levels in partially backfilled wells do not support this possibility.
6) The use of geochemical modeling to determine that cation exchange reactions are not likely to contribute to high radium levels in the downgradient, confined portion of the aquifer.
7) An investigation into colloidal transport of radium was undertaken. Elemental weight ratios of colloidal material indicate that colloids are primarily ferric oxide phases with lesser amounts of mixed layer illite/smectite. Direct measurement of radioactivity on these colloids indicates that they are not an important means of transporting radium in this aquifer.

References Cited

Beyerle, U., W. Aeschbach-Hertig, D. Imboden, H. Bauer, R. Kipfer 2000. A mass spectrometric system for the analysis of noble gas and tritium from water samples. Environ. Sci. Technol. 34: 2042-2050.

Bunn, R., R.Magelky, J. Ryan, and M. Elimelech. 2002. Mobilization of natural colloids from an iron oxide-coated sand aquifer: Effect of pH and ionic strength. Environ. Sci. Technol. 36(3): 314-322

CH2M Hill, Inc. 2000. Final results of selected mineralogical, petrographic and core analysis evaluations. Green Bay Wi. Aquifer Storage and Recovery Project. 107 pp.

Clayton, D. 1999. Determination of ^{238}U, ^{234}U, ^{232}Th, ^{230}Th and ^{226}Ra in the Maquoketa formation. M.S. thesis, Geosciences Department, University of Wisconsin-Milwaukee. 54 pp.

Cutler. P., D. MacAyeal, D. Mickelson, B. Parizek, and P. Colgan. 2000. Numerical simulation of ice-flow-permafrost interactions around the southern Laurentide ice sheet. J. Glaciol. 46:311-325.

Dansgaard, W. 1964. Stable isotopes in precipitation. Tellus 16 no. 4: 436-468.

Feinstein, D., D. Hart, T. Eaton, J. Krohelski, and K. Bradbury. 2005. Simulation of regional ground water flow in southeastern Wisconsin Report 2: Model results and interpretation. Southeastern Wisconsin Regional Planning Commission Technical Report 41. 63 pp.

Gilkeson, R.H., K. Cartwright, J.B. Cowart, and R.B. Holtzman.1983. Hydrogeologic and geochemical studies of selected natural radioisotopes and barium in ground water in Illinois. University of Illinois Water Resources Center, UILU-WRC-83-0180.

Gilkeson, R.H., and J.B. Cowart. 1982. A preliminary report on 238U series disequilibrium in ground water of the Cambrian-Ordovician Aquifer system of Northeastern Illinois. In Isotopic Studies of Hydrologic Processes. DeKalb, Illinois: Northern Illinois University Press.

Gilkeson, R.H., E.C. Perry, J.B. Cowart, and R.B. Holtzman. 1984. Isotopic studies of the natural sources of radium in ground water in Illinois. University of Illinois Water Resources Center, Urbana, Illinois, UILU WRC-84-187.

Gilkeson, R.H., S. Specht, K. Cartwright, and R.A. Griffen. 1978. Geologic studies to identify the source for high levels of radium and barium in Illinois ground water supplies. A preliminary report. Water Resources Center Report No. 78- 0135. Urbana-Champaign, Illinois: University of Illinois.

Grolimund, D., K. Barmettler, and M. Borkovec. 2001. Release and transport of colloidal particles in natural porous media, 2: Experimental results and effects of ligands. Water Resources Research 37, no. 3: 571–582.

Grundl, T. and M. Cape, 2006. Geochemical factors controlling radium activities in a sandstone aquifer. Groundwater 44, no. 4: 518-527.

Kipfer, R. , W. Aeschbach-Hertig, F. Peeters, and M. Stute. 2002. Nobel gases in lakes and groundwaters. Mineralogical Society of America Reviews in Mineralogy 47: 615-700.

Langmuir, D., and A. Riese. 1985. The thermodynamic properties of radium. Geochim et Cosmochim Acta 49, no. 7: 1593–1601.

Ma, L., M. Castro, C. Hall. 2004. A late Pleistocene-Holocene noble gas paleotemperature record in southern Michigan. Geoph. Res. Letters 31, L23204, 4 pp.

Mettler, S., M. Abdelmoula, E. Hoehn, R. Schoenenberger, P Weidler, and U. Von Gunten. Characterization of iron and manganese precipitates from an in-situ groundwater treatment plant. Ground Water 39 no 6.: 921-930.

Mickelson, D.M., L. Clayton, R.W. Baker, W.N. Mode, and A.F. Schneider. 1984. Pleistocene stratigraphic units of Wisconsin. Wisconsin Geological and Natural History Survey. Miscellaneous paper 84-1. 97 pp.

Moretti, G. 1971. Reference section for Paleozoic rocks in eastern Wisconsin: Van Driest #1, Sheboygan County. M.S. thesis, Geosciences Department, University of Wisconsin—Milwaukee. 127 pp.

Nicholas, J., M. Sherrill, and H. Young. 1984. Hydrogeology of the Cambro-Ordovician aquifer system at a test well in northeastern Illinois. U.S. Geological Survey Water-Resources Investigation 84-4165. USGS, Madison, Wisconsin.

Parkhurst, D.L. 1995. User's guide to PHREEQC—A computer program for speciation, reaction-path, advective-transport, and inverse geochemical calculations. USGS Water-Resources Investigations Report 95-4227. USGS, Reston, Virginia.

Perry, E.C., T. Grundl, R.Gilkeson H. 1982. H, O, and S isotopic study of the groundwater in the Cambrian-Ordovician aquifer system of northern Illinois in Isotope studies of hydrologic processes Perry, E.C. and C. Montgomery, eds., North. Ill. Univ. Press, DeKalb, IL, United States. Pp. 35-43.

Schmidt, L. 2002. Delineation of high salinity conditions in the Cambro-Ordovician aquifer of eastern Wisconsin. M.S. thesis, Geosciences Department, University of Wisconsin—Milwaukee. 58 pp.

Siegel, D.I. 1990. Sulfur isotope evidence for regional recharge of saline water during continental glaciation, North-Central United States. Geology 1990, no. 18: 1054–1056.

Soil Science Society America. 1982. Methods of soil analysis; Part 2, Chemical and microbiological properties; 2nd edition. Page, A L; Miller, R H; Keeney, D R, eds. p. 160.

Tachi, Y, T. Shibutani, H. Sato, M. Yui. 2001. Experimental and modeling studies on sorption and diffusion of radium in bentonite. J. Contaminant Hydrology, .47, no.2-4: 171-186.

USGS, 2006. Groundwater in the Great Lakes Basin, the case of southeast Wisconsin, Online website: http://wi.water.usgs.gov/glpf/

Winguth, C., D. Mickelson, P. Colgan, and B. Laabs. 2004. Modeling the deglaciation of the Green Bay lobeof the southern Laurentide ice sheet. Boreas 33:34-47.

Winter, B., C. Johnson, J. Simo and J. Valley. 1995. Paleozoic fluid history of the Michigan basin: Evidence from dolomite geochemistry in the middle Ordovician St Peter sandstone. J. Sedimentary Res. A65, no. 2:306-320.

WDNR. 2006. Wisconsin Department of Natural Resources Drinking Water System. Online database. http://www.dnr. state.wi.us/org/water/dwg/dws.htm.

Weaver, T.R., and J.M. Bahr. 1991a. Geochemical evolution in the Cambrian-Ordovician sandstone aquifer, Eastern Wisconsin: 1. Major ion and radionuclide distribution. Ground Water 29, no. 4: 350–356.

Weaver, T.R., and J.M. Bahr. 1991b. Geochemical evolution in the Cambrian-Ordovician sandstone aquifer, Eastern Wisconsin: 2. Correlation between flow paths and ground water chemistry. Ground Water 29, no. 4: 510–515.

WGNHS. 1995. Bedrock geology of Wisconsin. Wisconsin Geologic and Natural History Survey Map, Madison, Wisconsin.

Young, H.L. 1992.Summary of groundwater hydrology of the Cambro-Ordovician aquifer system in the northern Midwest, United States. United States Geological Survey Prof. Paper 1405-A. 55 pp.

Zhu, C. 2004. Co-precipitation in the barite isostructural family: Binary mixing properties. Geochim. et Cosmochim Acta 68,

APPENDIX A – Pewaukee 10 Solids Analysis

APPENDIX B – Noble Gas and Stable Isotope Data

NOBLE GAS AND STABLE ISOTOPE DATA FOR WAUKESHA COUNTY WELLS

NGT temps not reliable because of air contamination in the sample.

Wells in italics deliver water that is younger than the last glacial maximum.

Isotopic temperature is calculated from the global meteoric water line of Dansgaard, 1964.

WELL NAME	ABBREV.	WDNR unique well ID number	distance from Maquoketa outcrop	total depth	Noble gas temp.	deltaNe	delta ^{18}O	delta D	Isotopic temp.
			(km)	(ft)	(^{o}C)	(%)	(SMOW)	(SMOW)	(^{o}C)
Brookfield 10	BF-10	BH375	19	1635	5.5	air contamination	-12.65	-90.50	1.4
Brookfield 15	BF-15	BH380	21	1800	2.9	72	-11.40	-82.23	3.2
Delafield 1	DEL-1	IG412	3	1215	lost the noble gas sample		-10.12	-68.90	5.0
Dousman 1	*DOU-1*	*BH392*	*-1*	*1125*	*8.1*	*12.5*	*-9.37*	*-63.55*	*6.1*
Franklin 5	FR-5	BG451	39	1605	3.4	73.8	-9.35	-66.22	6.1
Jefferson 3	*JF-3*	*BG005*	*-23*	*838*	*5.6*	*20.9*	*-9.58*	*-63.57*	*5.8*
Mukwanogo 4	MUK-4	BH408	-1	1500	5.9	air contamination	-9.54	-68.77	5.8
Muskego 5	*MUS-5*	*IZ381*	*14*	*1400*	*4.2*	*20.1*	*-8.36*	*-60.64*	*7.5*
New Berlin 3	NB-3	BH411	23	1800	3.3	34.8	-9.91	-72.61	5.3
New Berlin 7	NB-7	BH415	26	2018	2.58	38	-9.67	-61.82	5.7
Pewaukee Village 4	*P-V4*	*BH423*	*8*	*1226*	*3.5*	*30.6*	*-9.94*	*-81.47*	*5.3*
Sussex 1	*SX-1*	*BH424*	*13*	*1298*	*4.5*	*30*	*-10.45*	*-79.54*	*4.5*
Waukesha 10	WK-10	BH436	15	2145	1.4	72	-12.32	-96.37	1.8
Waukesha 5	WK-5	BH431	18	2120	2.3	45.7	-12.00	-79.40	2.3
Waukesha 9 after backfilling	*WK-9*	*BH435*	*13*	*1725*	*5.6*	*28.3*	*-9.81*	*-62.47*	*5.5*

APPENDIX C – Major Ion and Radium Data